



NL 96 F 4 '94

NEW EUROPEAN CROSS-SECTION DATA LIBRARIES FOR ORIGEN-S BASED ON JEF2.2 AND EAF3

J.L. KLOOSTERMAN

The Netherlands Energy Research Foundation ECN is the leading institute in the Netherlands for energy research. ECN carries out basic and applied research in the fields of nuclear energy, fossil fuels, renewable energy sources, policy studies, environmental aspects of energy supply and the development and application of new materials.

ECN employs more than 900 staff. Contracts are obtained from the government and from national and foreign organizations and industries.

ECN's research results are published in a number of report series, each series serving a different public, from contractors to the international scientific world.

The R-series is for research reports that make the results of ECN research available to the international technical and scientific world.

Het Energieonderzoek Centrum Nederland (ECN) is het centrale instituut voor onderzoek op energiegebied in Nederland. ECN verricht fundamenteel en toegepast onderzoek op het gebied van kernenergie, fossiele-energie dragers, duurzame energie, beleidsstudies, milieuaspecten van de energievoorziening en de ontwikkeling en toepassing van nieuwe materialen.

Bij ECN zijn ruim 900 medewerkers werkzaam. De opdrachten worden verkregen van de overheid en van organisaties en industrieën uit binnen- en buitenland.

De resultaten van het ECN-onderzoek worden neergelegd in diverse rapportenseries, bestemd voor verschillende doelgroepen, van opdrachtgevers tot de internationale wetenschappelijke wereld.

De R-serie is de serie research-rapporten die de resultaten van ECN-onderzoek toegankelijk maken voor de internationale technisch-wetenschappelijke wereld.

Netherlands Energy Research Foundation ECN
P.O. Box 1
NL-1755 ZG Petten
the Netherlands
Telephone : +31 2246 49 49
Fax : +31 2246 44 80

This report is available on remittance of Dfl. 35 to:
ECN, General Services,
Petten, the Netherlands
Postbank account No. 3977703.
Please quote the report number.

© Netherlands Energy Research Foundation ECN

Energieonderzoek Centrum Nederland
Postbus 1
1755 ZG Petten
Telefoon : (02246) 49 49
Fax : (02246) 44 80

Dit rapport is te verkrijgen door het overmaken van f 35,- op girorekening 3977703 ten name van:
ECN, Algemene Diensten
te Petten
onder vermelding van het rapportnummer.

© Energieonderzoek Centrum Nederland

MARCH 1995



KS001923072

R: FI

DE008071573

ECN-R--95-008



DE008071573

NEW EUROPEAN CROSS-SECTION DATA LIBRARIES FOR ORIGEN-S BASED ON JEF2.2 AND EAF3

J.L. KLOOSTERMAN

Abstract

Cross-section data libraries for the ORIGEN-S fuel depletion code have been updated with cross sections from the JEF2.2 evaluated nuclear data file and the EAF3 activation file. For both an LWR and a LMFBR, cross-section data for 517 light elements, 65 actinides and 319 fission products have been renewed or added to the libraries (in total cross sections of 604 different nuclides).

The nuclides for which the cross sections have been updated were subdivided in two groups. One group of nuclides for which resonance shielding has been applied, and one group for which cross sections of nuclides at infinite dilution have been used. For the LWR, the first group consisted of 22 actinides and 32 fission products, for the LMFBR this group contained 22 actinides (the same as for the PWR) and 26 fission products.

For the LWR, the French PWR-N4 reactor was used as a reference design. Spectrum-integrated cross sections of nuclides in the first group (with corrections for resonance shielding) have been calculated as a function of burnup, and the cross sections at average burnup have been used to update the libraries. Spectrum-integrated cross sections of all other nuclides (without resonance shielding corrections), have been obtained with the neutron spectrum at average burnup, and the few-group cross sections have been used to update the libraries.

For the LMFBR, the Superphénix fast reactor was used as a reference design. Also for this reactor, the nuclide cross sections have been calculated as a function of burnup, but the burnup dependence of these cross sections turned out to be very small. The procedures for both nuclide groups were similar to those of the LWR.

The new cross-section data libraries have been validated by several test runs. From these calculations it is concluded that despite the new cross sections, regular updates of the cross sections during the burnup sequence remain necessary for the most important actinides and fission products in order to account for the burnup dependence of the cross sections of these nuclides. This is especially so for the LWR. For all other nuclides, the cross sections of the new ORIGEN-S libraries can be used.

Keywords

Actinides
Burnup
Cross sections
Data libraries
Fission products
Fuel depletion
Light elements
Transmutation

This work has been performed in the framework of a contract with the European Union ("Participation in a CEC strategy study on nuclear waste transmutation") under contract number F12W-CT-91-0104 (ECN project number 1115.62).

CONTENTS

1. INTRODUCTION	5
1.1 Introduction	5
1.2 ORIGEN-S	5
1.3 Contents of the libraries	8
2. DEFINITION OF CROSS SECTIONS	9
2.1 Introduction	9
2.2 Light Element Library	9
2.3 Actinide Library	10
2.4 Fission Product Library	10
3. UPDATE WITH JEF2.2 CROSS SECTIONS	14
3.1 Introduction	14
3.2 Calculations and results on the LWR	17
3.2.1 Design data LWR	17
3.2.2 Results of the burnup calculations	18
3.2.3 Resultant cross sections	24
3.3 Calculations and results on the LMFBR	28
3.3.1 Design data LMFBR	28
3.3.2 Results	28
4. UPDATE WITH EAF3 CROSS SECTIONS	31
4.1 Update of cross sections	31
4.2 Update of isomer ratios	31
5. VALIDATION OF THE NEW LIBRARIES	33
5.1 Calculations on the PWR-N4	33
5.2 Calculations on the burnup credit criticality benchmark	34
5.3 Calculations on Superphénix	34
6. CONCLUSIONS	40
7. ACKNOWLEDGEMENTS	41
REFERENCES	42
APPENDIX A. LIST OF SYMBOLS	43
APPENDIX B. ORIGIN OF CROSS SECTIONS	44

1. INTRODUCTION

1.1 Introduction

In calculational studies on transmutation of actinides, many data are used of which the most important ones are cross sections, half lives and branching fractions for decay. Often, these data are based on rather old data files. In this report, an update of cross sections in the data libraries of the ORIGEN-S [1] fuel depletion code is described. This work has already been reported shortly in reference [2]. The update of decay data and fission product yields together with a summary of this report will be presented elsewhere [3].

1.2 ORIGEN-S

ORIGEN-S is a general multi-purpose fuel depletion code, which is often used in fuel burnup calculations and transmutation studies. It uses data from three cross-section data libraries in readable ASCII format (one library for light elements, one library for actinides and one library for fission products; see also section 2.1) [4], or it uses one data library in binary format. This binary library can be made by converting the three ASCII libraries into one binary library by means of the code COUPLE [5].

There are a few important differences between the cross-section data in the ASCII libraries and in the binary library. The three ASCII libraries contain cross-section data for four different reactor types, while the binary library contains one-group cross-section data for only one reactor type. The four reactor types are: a High Temperature Gas-cooled Reactor (HTGR), a Light Water Reactor (LWR), a Liquid Metal-cooled Fast Breeder Reactor (LMFBR), and a Molten Salt Breeder Reactor (MSBR). In contrast to the binary library, the cross sections in the ASCII libraries for the thermal reactor types (HTGR, LWR and MSBR) are given in three energy groups (a cross section at thermal energy σ_0 , a resonance integral I , and a fission-spectrum-averaged cross section σ_1); these groups are condensed by ORIGEN-S into one group by means of three spectral parameters. The above mentioned spectral parameters are called THERM, RES and FAST, and are also used by the COUPLE code to convert the three ASCII libraries into one binary library. One-group cross sections for the thermal reactors are given per unit of *thermal* neutron flux. For the LMFBR, both the ASCII libraries and the binary library contain only one-group cross sections per unit of *total* neutron flux.

Each of the spectral parameters mentioned above has a plain physical meaning. THERM is used to convert cross sections at thermal energy to a cross section averaged over the total thermal neutron flux ($E < 0.5$ eV). It is equal to the ratio of the thermal reaction rate of a nuclide with a $1/v$ absorption cross section and the product of its thermal cross section and the actual thermal neutron flux. This gives:

$$\text{THERM} = \frac{\sqrt{E_0} \int_0^{0.5} \phi(E) / \sqrt{E} dE}{\int_0^{0.5} \phi(E) dE} \approx \sqrt{\frac{\pi T_0}{4 T}} \quad (1.1)$$

where the approximation holds for a Maxwellian neutron spectrum with energy below 0.5 eV.

RES is used to normalize the resonance integral I to get a proper epithermal neutron cross section, and to convert this cross section to the epithermal reaction rate per unit of thermal neutron flux:

$$\text{RES} = \left[\int_{0.5}^{10^6} \frac{1}{E} dE \right]^{-1} \frac{\phi_{\text{res}}}{\phi_{\text{trm}}} = [\ln(2 \cdot 10^6)]^{-1} \frac{\phi_{\text{res}}}{\phi_{\text{trm}}} \quad (1.2)$$

FAST is used to convert fission-spectrum-averaged cross sections σ_1 to cross sections properly averaged over the fast energy region and to calculate the fast reaction rate per unit of thermal neutron flux:

$$\text{FAST} = \frac{\int_0^{\infty} \phi_{\text{fis}}(E) dE}{\int_{10^6}^{\infty} \phi_{\text{fis}}(E) dE} \frac{\phi_{\text{fst}}}{\phi_{\text{trm}}} \approx 1.45 \frac{\phi_{\text{fst}}}{\phi_{\text{trm}}} \quad (1.3)$$

ORIGIN-S can be used either as a stand-alone module or within the SCALE package. In the first case, the three ASCII libraries can be used or the single binary library. In the second case, other modules from the SCALE package are used to calculate properly resonance-shielded cross sections and to average these cross sections over the fuel region of the reactor of interest. This is schematically shown in figure 1.1, where the two pictures on the left hand side (pictures A and B) show the procedure for calculations with ORIGIN-S as a stand-alone module, and the figure on the right hand side (picture C) shows the scheme when ORIGIN-S is used within the SCALE package. In that case the one-group cross sections in the binary library are updated with cross sections from the spectrum calculation. This update is also done by the COUPLE code as will be explained later on in section 3.1 (see figure 3.1). The fact that the cross sections in the binary library can be updated is probably the most important reason to use one library in binary format instead of three libraries in ASCII format.

The advantage of using ORIGIN-S as a stand-alone module rather than the frequently used ORIGEN2 code (or versions of it), is that whereas ORIGEN2 requires pre-calculated one-group cross sections, ORIGIN-S offers more flexibility for thermal reactor calculations, because it uses three-group cross sections which are condensed to one group by means of the above mentioned spectral parameters. Users of ORIGIN-S are supposed to overwrite those cross sections which are strongly dependent on burnup (e.g. due to resonance shielding or spectrum shifts). In particular, this is important for actinides and some fission products.

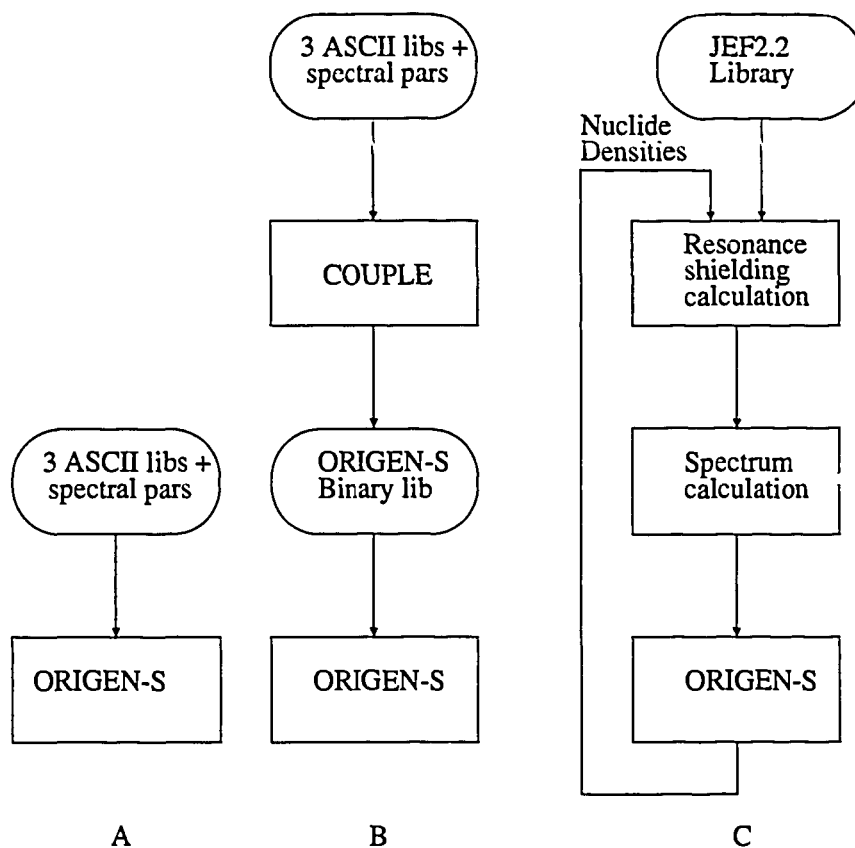


Figure 1.1 Scheme of burnup calculations with *ORIGEN-S* as a stand alone module (pictures A and B) or with *ORIGEN-S* within the *SCALE* package (picture C).

1.3 Contents of the libraries

The libraries in ASCII format contain for each nuclide one record with decay data and four records with cross-section data and fission-products yields [4]. The decay-data record contains:

- Half lives.
- Branching fractions (fraction for β^- decay to metastable state, β^+ decay, β^+ decay to metastable state, α decay, isomeric transition, and spontaneous fission).
- Recoverable energy per decay and the fraction of this energy that comes from γ rays.
- Radioactivity concentration guides for ingestion and inhalation. These parameters are not used anymore, because the radiotoxicity of a radioisotope is now defined by guidelines of the ICRP [6].

The cross-section records contain thermal cross sections (σ_0), resonance integrals (I), and fission-spectrum-averaged cross sections (σ_1). Also the isomer ratios (measures of the chance that nuclides are produced in a metastable state) are given in these records. As mentioned in the previous section, all cross sections are given for four reactor types: an HTGR, an LWR, a LMFBR and a MSBR. Fission-product yields are given in the cross-section records of the library which contains data for fission products. The definitions of the cross sections in the ORIGEN-S libraries are given in chapter 2. In this work, cross-section updates have only been made for an LWR and a LMFBR. For the HTGR and the MSBR, the user is supposed to overwrite those cross sections which are strongly dependent on burnup (e.g. cross sections of most actinides and some fission products).

Cross sections in the ORIGEN-S libraries are updated with data as much as possible based on the Joint Evaluated File version 2.2 (JEF2.2). Because the ORIGEN-S libraries contain data for more nuclides than present in the JEF2.2 file, cross sections from nuclides not present in the JEF2.2 file were taken from the European Activation File version 3 (EAF3) [7], which is a very extensive file containing cross sections for 729 target nuclides with half lives larger than 0.5 day. Also the isomer ratios (measures of the chance that nuclides are produced in a metastable state) have been updated using the information given in the EAF3 file.

Other data in the ORIGEN-S data libraries (e.g. half lives, Q-values and fission product yields) have also been updated based on the JEF2.2 file. This is described elsewhere [3].

2. DEFINITION OF CROSS SECTIONS

2.1 Introduction

As explained in section 1.1, the ORIGEN-S fuel depletion code uses three different ASCII libraries or one binary library. In the latter case, the three ASCII libraries are converted into one binary library by the COUPLE code prior to the actual burnup calculations. The three different ASCII libraries contain data for the light elements, the actinides, and for the fission products.

The light element library originally contained data for either 253 or 674 elements, with atomic numbers ranging from 1 to 84. The cross sections in this library are specially designed to calculate activation rates and products. In the remainder of this report, we will always refer to the large light element library originally containing 674 elements, unless otherwise stated.

The actinide library originally contained data for 101 actinides and decay daughter products with atomic numbers ranging from 81 to 99.

The fission product library, finally, originally contained data for either 461 or 821 fission products with atomic numbers ranging from 27 to 68. For the elements in this library, only a few cross sections are given and five fission product yields for five different actinide isotopes. In the remainder of this report, we will always refer to the large fission product library originally containing data for 821 elements, unless otherwise stated.

During the update procedure, the number of nuclides in the three data libraries have been increased. For some new nuclides added to the libraries, only the decay-data record is given because no cross sections were available. The new nuclides in the three different libraries for which also cross-section data have been added are listed in Appendix B, together with the nuclides which were already present in the libraries, and for which the cross-section data have also been updated.

The meaning of the cross sections in the libraries depends on the reactor type for which the data is given. As mentioned in section 1.2, cross sections are given for four different reactor types: an HTGR, an LWR, a LMFBF, and a MSBR. The cross-section updates have only been performed for the LWR and the LMFBF.

2.2 Light Element Library

The cross-section data in the light element library is explained in words in table 2.1, and in mathematical equations in table 2.2. The meaning as given in table 2.2 is used for the update of the cross sections as described in chapters 3 and 4. In ORIGEN-S, cross-section fractions and one-group cross sections are calculated from the cross sections in table 2.2 according to the definitions given in table 2.3. For the LMFBFs, the spectral parameters THERM, RES and FAST are not used and have always values equal to one, because for this reactor type one-group cross sections are already given in the library. The σ_γ and σ_{2n} from table 2.3 are subdivided in two cross sections each; one for the creation of a product nuclide in the ground state, and one for the creation of a product nuclide in a metastable state. This is done by means of the isomer ratios FNG1 and FN2N1 given in tables 2.1 and 2.2.

2.3 Actinide Library

The cross-section data in the actinide library is explained in words in table 2.4, and in mathematical equations in table 2.5. Again, the meaning as given in table 2.5 is used for the update of the cross sections as described in chapters 3 and 4. In ORIGEN-S one-group cross sections are calculated from the cross sections in table 2.5 according to the definitions given in table 2.6. For the LMFBRs, the spectral parameters THERM, RES and FAST are not used and have always values equal to one, because for this reactor type one-group cross sections are already given in the library. As for the light element library, the σ_γ and σ_{2n} are subdivided in two cross sections each; one for the creation of a product nuclide in the ground state, and one for the creation of a product nuclide in a metastable state. This is done by means of the isomer ratios FNG1 and FN2N1 given in tables 2.4 and 2.5.

2.4 Fission Product Library

The fission product library contains only the cross sections SIGNG and RING and the isomer ratio FNG1, which have the same meaning as in the actinide library (see tables 2.4 and 2.5). Only the σ_γ cross section is calculated according to the definition in table 2.6, and can again be subdivided in two cross sections by means of the isomer ratio FNG1 given in tables 2.4 and 2.5.

Table 2.1 *Meaning of the cross sections in the light element library for HTGRs, LWRs and MSBRs. The meaning of these cross sections for LMFBRs becomes clear from table 2.2.*

Cross section	Description
SIGTH	Thermal cross section for total neutron absorption ($E = 0.0253$ eV).
FNG1	Isomer ratio for (n, γ) reaction (fraction of (n, γ) cross section that produces a nuclide in a metastable state.
FNA	Fraction of SIGTH that produces (n, α) reactions.
FNP	Fraction of SIGTH that produces (n,p) reactions.
RITH	Resonance integral for epithermal neutron absorption.
FINA	Fraction of RITH that produces (n, α) reactions.
FINP	Fraction of RITH that produces (n,p) reactions.
SIGMEV	Fission-spectrum-averaged cross section for reactions with threshold energy above 1 MeV.
FN2N1	Isomer ratio for (n,2n) reaction (fraction of (n,2n) cross section that produces a nuclide in a metastable state.
FFNA	Fraction of SIGMEV that produces (n, α) reactions.
FFNP	Fraction of SIGMEV that produces (n,p) reactions.

Table 2.2 *Meaning of the cross sections in the light element library.*

Cross section	HTGR, LWR and MSBR	LMFBR
SIGTH	$\frac{\int_0^{0.5} \sigma_a(E) \phi(E) dE}{\int_0^{0.5} \phi(E) dE} \cdot \frac{1}{\text{THERM}}$	$\frac{\int_0^{\infty} \sigma_a(E) \phi(E) dE}{\int_0^{\infty} \phi(E) dE}$
FNG1	$\frac{\int_0^{\infty} (\sigma_\gamma^1(E) + \sigma_\gamma^2(E)) \phi(E) dE}{\int_0^{\infty} \sigma_\gamma(E) \phi(E) dE}$	$\frac{\int_0^{\infty} (\sigma_\gamma^1(E) + \sigma_\gamma^2(E)) \phi(E) dE}{\int_0^{\infty} \sigma_\gamma(E) \phi(E) dE}$
FNA	$\frac{\int_0^{0.5} \sigma_a(E) \phi(E) dE}{\int_0^{0.5} \sigma_a(E) \phi(E) dE}$	0
FNP	$\frac{\int_0^{0.5} \sigma_p(E) \phi(E) dE}{\int_0^{0.5} \sigma_p(E) \phi(E) dE}$	0
RITH	$\frac{\int_0^{0.5} \sigma_\gamma(E) \phi(E) dE + \int_{0.5}^{10^6} (\sigma_p(E) + \sigma_a(E)) \phi(E) dE}{\int_{0.5}^{10^6} \phi(E) dE / \ln(2 \cdot 10^6)}$	0
FINA	$\frac{\int_{0.5}^{10^6} \sigma_a(E) \phi(E) dE}{\int_{0.5}^{\infty} \sigma_\gamma(E) \phi(E) dE + \int_{0.5}^{10^6} (\sigma_p(E) + \sigma_a(E)) \phi(E) dE}$	0
FINP	$\frac{\int_{0.5}^{10^6} \sigma_p(E) \phi(E) dE}{\int_{0.5}^{\infty} \sigma_\gamma(E) \phi(E) dE + \int_{0.5}^{10^6} (\sigma_p(E) + \sigma_a(E)) \phi(E) dE}$	0
SIGMEV	$\frac{\int_0^{\infty} \sigma_{2n}(E) \phi(E) dE + \int_{10^6}^{\infty} (\sigma_p(E) + \sigma_a(E)) \phi(E) dE}{1.45 \int_{10^6}^{\infty} \phi(E) dE}$	$\frac{\int_0^{\infty} (\sigma_{2n}(E) + \sigma_p(E) + \sigma_a(E)) \phi(E) dE}{\int_0^{\infty} \phi(E) dE}$
FN2N1	$\frac{\int_{10^6}^{\infty} (\sigma_{2n}^1(E) + \sigma_{2n}^2(E)) \phi(E) dE}{\int_{10^6}^{\infty} \sigma_{2n}(E) \phi(E) dE}$	$\frac{\int_0^{\infty} (\sigma_{2n}^1(E) + \sigma_{2n}^2(E)) \phi(E) dE}{\int_0^{\infty} \sigma_{2n}(E) \phi(E) dE}$
FFNA	$\frac{\int_{10^6}^{\infty} \sigma_a(E) \phi(E) dE}{\int_0^{\infty} \sigma_{2n}(E) \phi(E) dE + \int_{10^6}^{\infty} (\sigma_p(E) + \sigma_a(E)) \phi(E) dE}$	$\frac{\int_0^{\infty} \sigma_a(E) \phi(E) dE}{\int_0^{\infty} (\sigma_{2n}(E) + \sigma_p(E) + \sigma_a(E)) \phi(E) dE}$
FFNP	$\frac{\int_{10^6}^{\infty} \sigma_p(E) \phi(E) dE}{\int_0^{\infty} \sigma_{2n}(E) \phi(E) dE + \int_{10^6}^{\infty} (\sigma_p(E) + \sigma_a(E)) \phi(E) dE}$	$\frac{\int_0^{\infty} \sigma_p(E) \phi(E) dE}{\int_0^{\infty} (\sigma_{2n}(E) + \sigma_p(E) + \sigma_a(E)) \phi(E) dE}$

Table 2.3 *Fractions and one-group cross sections derived from the cross sections in the ORIGEN-S light element library as given in table 2.2.*

Cross section	Description
FNG	1.0 - FNA - FNP
FING	1.0 - FINA - FINP
FN2N	1.0 - FFNA - FFNP
σ_γ	THERM·SIGTH·FNG + RES·RITH·FING
σ_a	THERM·SIGTH·FNA + RES·RITH·FINA + FAST·SIGMEV·FFNA
σ_p	THERM·SIGTH·FNP + RES·RITH·FINP + FAST·SIGMEV·FFNP
σ_{2n}	FAST·SIGMEV·FN2N

Table 2.4 *Meaning of the cross sections in the actinide library for HTGRs, LWRs, and MSBRs. The meaning of these cross sections for LMFBRs becomes clear from table 2.5.*

Cross section	Description
SIGNG	Thermal cross section for (n,γ) reactions ($E = 0.0253$ eV).
RING	Resonance integral for (n,γ) reactions.
FNG1	Isomer ratio for (n,γ) reaction (fraction of (n,γ) cross section that produces a nuclide in a metastable state).
SIGF	Thermal cross section for (n,f) reactions ($E = 0.0253$ eV).
RIF	Resonance integral for (n,f) reactions.
SIGFF	Fission-spectrum-averaged (n,f) cross section for reactions with threshold energy above 1 MeV.
SIGN2N	Fission-spectrum-averaged (n,2n) cross section.
FN2N1	Isomer ratio for (n,2n) reaction (fraction of (n,2n) cross section that produces a nuclide in a metastable state).
SIGN3N	Fission-spectrum-averaged (n,3n) cross section.

 Table 2.5 *Meaning of the cross sections in the actinide library.*

Cross section	HTGR, LWR and MSBR	LMFBR
SIGNG	$\frac{\int_0^{0.5} \sigma_\gamma(E) \phi(E) dE}{\int_0^{0.5} \phi(E) dE} \text{ THERM}$	$\frac{\int_0^\infty \sigma_\gamma(E) \phi(E) dE}{\int_0^\infty \phi(E) dE}$
RING	$\frac{\int_{0.5}^\infty \sigma_\gamma(E) \phi(E) dE}{\int_{0.5}^{10^6} \phi(E) dE} \ln(2 \cdot 10^6)$	0
FNG1	$\frac{\int_0^\infty (\sigma_\gamma^1(E) + \sigma_\gamma^2(E)) \phi(E) dE}{\int_0^\infty \sigma_\gamma(E) \phi(E) dE}$	$\frac{\int_0^\infty (\sigma_\gamma^1(E) + \sigma_\gamma^2(E)) \phi(E) dE}{\int_0^\infty \sigma_\gamma(E) \phi(E) dE}$
SIGF	$\frac{\int_0^{0.5} \sigma_f(E) \phi(E) dE}{\int_0^{0.5} \phi(E) dE} \text{ THERM}$	$\frac{\int_0^\infty \sigma_f(E) \phi(E) dE}{\int_0^\infty \phi(E) dE}$
RIF	$\frac{\int_{0.5}^{10^6} \sigma_f(E) \phi(E) dE}{\int_{0.5}^{10^6} \phi(E) dE} \ln(2 \cdot 10^6)$	0
SIGFF	$\frac{\int_{10^6}^\infty \sigma_f(E) \phi(E) dE}{\int_{10^6}^\infty \phi(E) dE} \frac{1}{1.45}$	0
SIGN2N	$\frac{\int_0^\infty \sigma_{2n}(E) \phi(E) dE}{\int_{10^6}^\infty \phi(E) dE} \frac{1}{1.45}$	$\frac{\int_0^\infty \sigma_{2n}(E) \phi(E) dE}{\int_0^\infty \phi(E) dE}$
FN2N1	$\frac{\int_0^\infty (\sigma_{2n}^1(E) + \sigma_{2n}^2(E)) \phi(E) dE}{\int_0^\infty \sigma_{2n}(E) \phi(E) dE}$	$\frac{\int_0^\infty (\sigma_{2n}^1(E) + \sigma_{2n}^2(E)) \phi(E) dE}{\int_0^\infty \sigma_{2n}(E) \phi(E) dE}$
SIGN3N	$\frac{\int_0^\infty \sigma_{3n}(E) \phi(E) dE}{\int_{10^6}^\infty \phi(E) dE} \frac{1}{1.45}$	$\frac{\int_0^\infty \sigma_{3n}(E) \phi(E) dE}{\int_0^\infty \phi(E) dE}$

Table 2.6 *Fractions and one-group cross sections derived from the cross sections in the actinide library as given in table 2.5.*

Cross section	Description
σ_γ	THERM·SIGNG + RES·RING
σ_f	THERM·SIGF + RES·RIF + FAST·SIGFF
σ_{2n}	FAST·SIGN2N
σ_{3n}	FAST·SIGN3N

3. UPDATE WITH JEF2.2 CROSS SECTIONS

3.1 Introduction

Many cross sections in the ORIGEN-S data libraries have been updated with cross-section data from the JEF2.2 evaluated nuclear data file. For this purpose, the ECN cross-section data library in XMAS-group structure has been used. This library contains data based on JEF2.2 for about 275 actinide isotopes, light elements and fission products, and has been processed by NJOY89.62 [8].

The nuclides in above mentioned ECN-XMAS library have been divided in two groups: one group of nuclides for which resonance shielding has been accounted for (about 50 nuclides), and one group for which cross sections at infinite dilution have been used (about 225 nuclides).

The first group of nuclides was used to calculate the neutron spectra of the LWR and the LMFBR as a function of burnup. A list of these nuclides is given in table 3.1. For many nuclides in this table, resonance shielding calculations were done as a function of burnup with the Bondarenko shielding method in the unresolved energy region by the BONAMI-4 code [9], and with the Nordheim shielding method in the resolved energy region by the NITAWL-4 code [10] (although resonance parameters were not available for all nuclides in this table).

The burnup calculations were done with the SCALE code system according to the scheme shown in figure 3.1. As explained above, the BONAMI-4 and NITAWL-4 codes were used for resonance shielding calculations, XSDNRNPM-S [11] was used to calculate the pin-cell averaged cross sections of all isotopes, and to condense these cross sections to three groups for the LWR or to one group for the LMFBR, COUPLE was used to update the binary ORIGEN-S library with these few-group cross sections, and ORIGEN-S itself was used to calculate the nuclide densities in the fuel pin at the following time step. With these new nuclide densities, the calculational sequence has been repeated until the requested fuel burnup has been reached. The results of these calculations are the neutron spectra of the LWR and the LMFBR as a function of burnup, and the three-group and one-group cross sections of these 50 nuclides as a function of burnup. The above mentioned three-group cross sections for the LWR and the one-group cross sections for the LMFBR at average burnup were converted to ORIGEN-S format according to tables 2.2 and 2.5 by means of a conversion program.

The second group of nuclides consisted of all other nuclides (about 225), and the fine-group cross sections of these nuclides were collapsed to three groups for the LWR and to one group for the LMFBR by use of the fine-group neutron fluxes in the fuel region at average burnup of the reactor under consideration. These cross sections were also converted to ORIGEN-S format according to tables 2.2 and 2.5 by the same conversion program as used for the resonance-shielded cross sections.

The update procedure is schematically shown in figure 3.2 (branch on the left hand side of the figure).

Table 3.1 *The list of actinide isotopes and fission products accounted for in the fuel pin cell calculations. The actinides selected were the same for both the LWR and the LMFBP.*

Number	Actinides	Fission products	
		LWR	LMFBR
1	^{234}U	^{83}Kr	^{93}Zr
2	^{235}U	^{93}Zr	^{95}Zr
3	^{236}U	^{95}Mo	^{95}Mo
4	^{238}U	^{99}Tc	^{97}Mo
5	^{237}Np	^{101}Ru	^{98}Mo
6	^{238}Np	^{103}Rh	^{100}Mo
7	^{239}Np	^{105}Rh	^{99}Tc
8	^{238}Pu	^{109}Ag	^{101}Ru
9	^{239}Pu	^{113}Cd	^{103}Ru
10	^{240}Pu	^{127}I	^{104}Ru
11	^{241}Pu	^{129}I	^{103}Rh
12	^{242}Pu	^{131}Xe	^{107}Pd
13	^{243}Pu	^{135}Xe	^{109}Ag
14	^{241}Am	^{133}Cs	^{127}I
15	^{242}Am	^{134}Cs	^{129}I
16	^{242m}Am	^{135}Cs	^{131}Xe
17	^{243}Am	^{139}La	^{133}Cs
18	^{242}Cm	^{141}Pr	^{135}Cs
19	^{243}Cm	^{143}Nd	^{141}Pr
20	^{244}Cm	^{146}Nd	^{143}Nd
21	^{245}Cm	^{147}Pm	^{145}Nd
22	^{246}Cm	^{148}Pm	^{147}Pm
23		^{148m}Pm	^{149}Sm
24		^{149}Pm	^{151}Sm
25		^{147}Sm	^{153}Eu
26		^{149}Sm	^{155}Eu
27		^{150}Sm	
28		^{151}Sm	
29		^{152}Sm	
30		^{153}Eu	
31		^{154}Eu	
32		^{155}Eu	

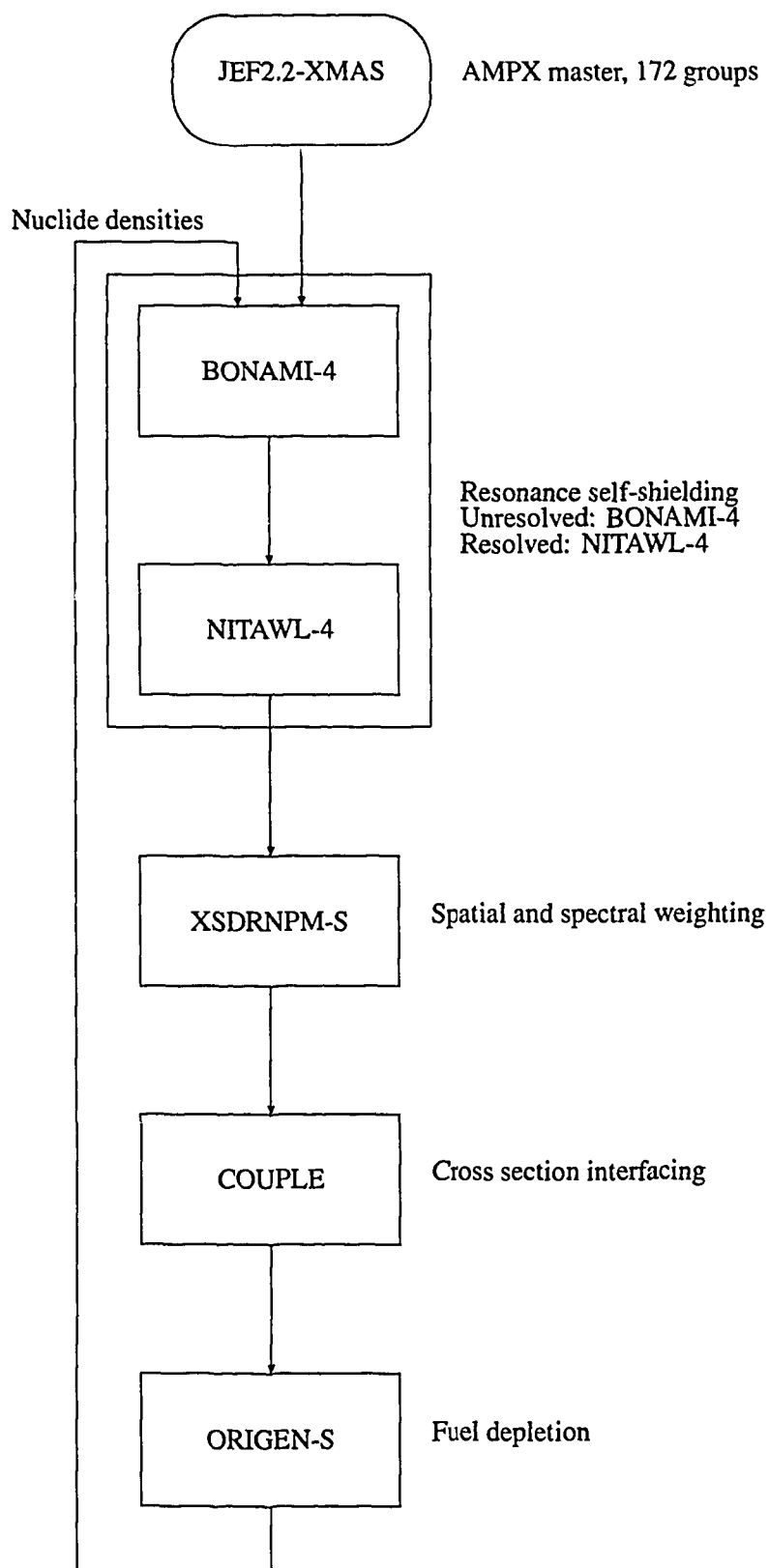


Figure 3.1 Scheme of the rigorous burnup calculations with the SCALE code package with regular cross section updating.

3.2 Calculations and results on the LWR

3.2.1 Design data LWR

The French PWR-N4 was used as a reference design for the burnup calculation on the LWR. Design data were kindly provided by CEA, and are tabulated in table

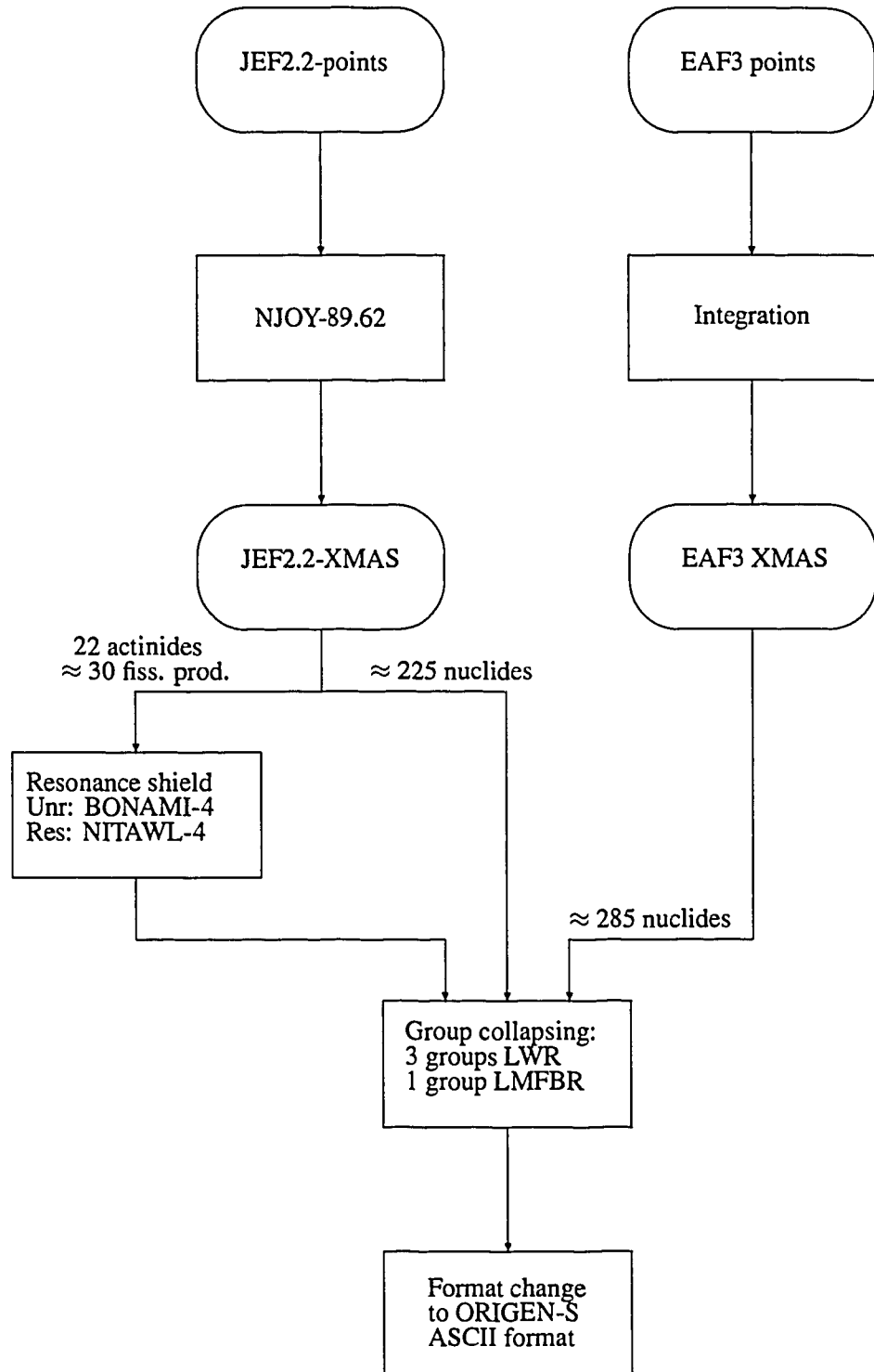


Figure 3.2 Scheme of the update of the ORIGIN-S libraries in ASCII format.

3.2. The cross sections in the ORIGIN-S library were updated six times during the burnup sequence. The boron concentration in the moderator was supposed to be linearly dependent on burnup and was varied from 1000 ppm at begin of cycle (BOC) to zero at end of cycle (EOC). This is expected to give a slightly harder cycle-averaged neutron spectrum than would be obtained with a fixed boron concentration [12].

Table 3.2 *Design data for the burnup calculations on the PWR-N4.*

Geometrical data (cm)	
Fuel outer radius	0.41266
Clad outer radius	0.47436
Lattice pitch	1.32484
Temperatures (K)	
Fuel	930
Clad	586
Moderator	586
Nuclide densities in the fuel at BOL ($\text{barn}^{-1}\text{cm}^{-1}$)	
^{234}U	7.3094E-06
^{235}U	9.0977E-04
^{238}U	2.1552E-02
^{16}O	4.4937E-02
Nuclide densities in the cladding ($\text{barn}^{-1}\text{cm}^{-1}$)	
^{nat}Zr	4.3088E-02
^{nat}Cr	9.6379E-05
^{nat}Fe	1.5777E-04
Nuclide densities in the moderator at BOC ($\text{barn}^{-1}\text{cm}^{-1}$)	
^1H	4.6644E-02
^{16}O	2.3322E-02
^{10}B	7.6864E-06
^{11}B	3.1173E-05
Burnup data	
Initial enrichment (wt%)	4.0
Number of cycles	5
Burnup per cycle (MWd/tU)	9500
Maximum burnup (MWd/tU)	47500
Number of EFPD per cycle	262
Cooling time per cycle (day)	102
Specific power (MWth/tU)	36.26
Boron concentration (ppm)	1000-0
Number of cell calculations per cycle	6
Number of cell calculations in total	30
Number of actinides in cell	22
Number of fission products in cell	32

3.2.2 Results of the burnup calculations

The k_{∞} as a function of burnup is given in figure 3.3. It is seen that at the beginning of each cycle with burnup of 9.5 GWd/tU, the k_{∞} drops significantly due to the boron concentration which is set to 1000 ppm at BOC, and which is assumed to decrease linearly to zero at EOC. After the first pass in each cycle, the k_{∞} drops also due to the buildup of xenon and other short-lived fission products (recall that

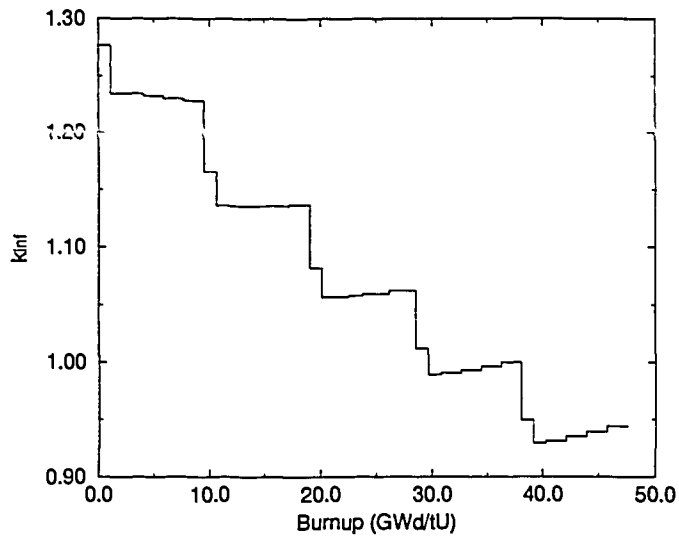


Figure 3.3 The infinite multiplication factor for the PWR-N4 as a function of burnup.

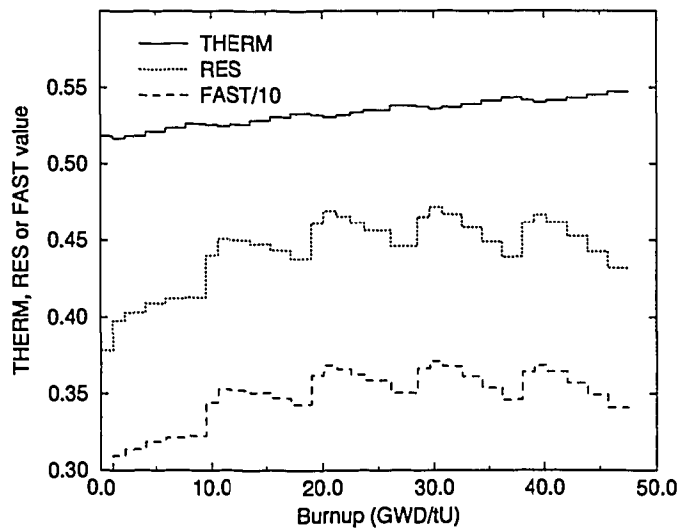


Figure 3.4 The three spectral parameters THERM, RES and FAST for the PWR-N4 as a function of burnup.

after each burnup cycle a cooling period of 102 days is modelled during which these fission products decay). In figure 3.3, it is seen that the decrease of the boron concentration during the last three cycles has a larger reactivity effect than the depletion of fissile material and the buildup of fission products during these cycles.

The three spectral parameters THERM, RES and FAST are shown in figure 3.4 as a function of burnup, where it is noted that the FAST values are divided by ten to obtain a well-scaled figure. From this figure several trends can be noticed.

First, the value of THERM increases as a function of burnup, which means that the thermal neutron flux becomes softer with increasing burnup. This is mainly due to the buildup of ^{239}Pu which has a large resonance at 0.3 eV, and to a lesser extend

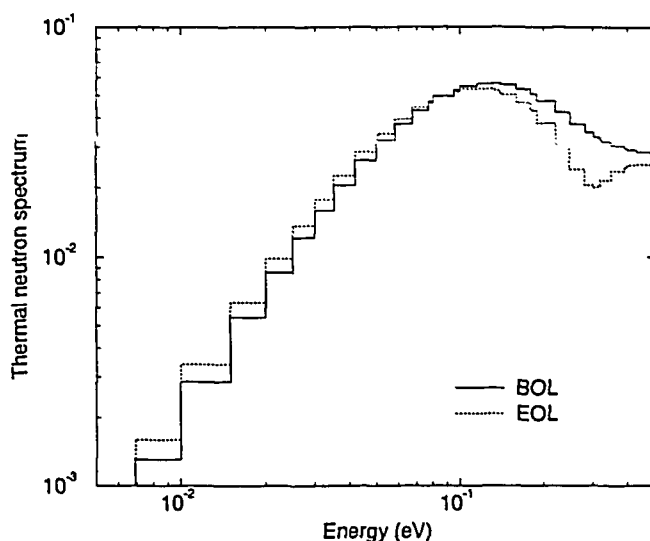


Figure 3.5 The spectrum of the thermal neutron flux at BOL and at EOL for the PWR-N4. The thermal neutron flux in both cases is normalized to unity.

to the buildup of ^{240}Pu which has a large resonance at 1.0 eV. Buildup of these two plutonium isotopes leads to a softening of the thermal neutron flux below 0.5 eV, as can be seen in figure 3.5. Also the decrease of the boron concentration during each cycle leads to a softening of the thermal neutron flux, because ^{10}B has a high absorption cross section with a $1/v$ energy dependence in this energy region ($E < 0.5$ eV). However, this effect is partly compensated by buildup of ^{135}Xe and other fission products.

Secondly, the values of RES and FAST tend to increase during the first three burnup cycles, while they decrease during the fourth and fifth burnup cycles. From equations 1.2 and 1.3 follows that RES is proportional to the ratio of the resonance and the thermal flux, and that FAST is proportional to the ratio of the fast and thermal flux. The burnup dependencies of the RES and FAST parameters are mainly due to variations in the thermal neutron flux relative to the resonance and fast neutron fluxes. This is seen in figure 3.6 where the thermal flux, the resonance flux divided by ten (to obtain a well-scaled figure) and the fast neutron flux are given per fission neutron produced. It must be noted that from this figure should not be concluded that the fast and resonance fluxes remain constant during the irradiation, and that only the thermal flux changes. The actual values of the three-group fluxes depend on the burnup and the power density of the fuel. For example, if the power density in the fuel is kept constant during the burnup sequence, the thermal neutron flux is expected to increase monotonously as a function of irradiation time to compensate for the depletion of the fuel (such that the product of the macroscopic fission cross section and the thermal neutron flux remains almost constant during the burnup sequence). The actual power density in the fuel is dependent on the burnup and is mainly determined by the fuel management scheme applied.

From figure 3.6 can be seen that the spectrum hardens during the first three burnup cycles, and that it softens again during the last two cycles. This is mainly due to changing macroscopic cross sections in the fuel region. The macroscopic cross sections in the resonance energy range are shown in figure 3.7, and in the thermal

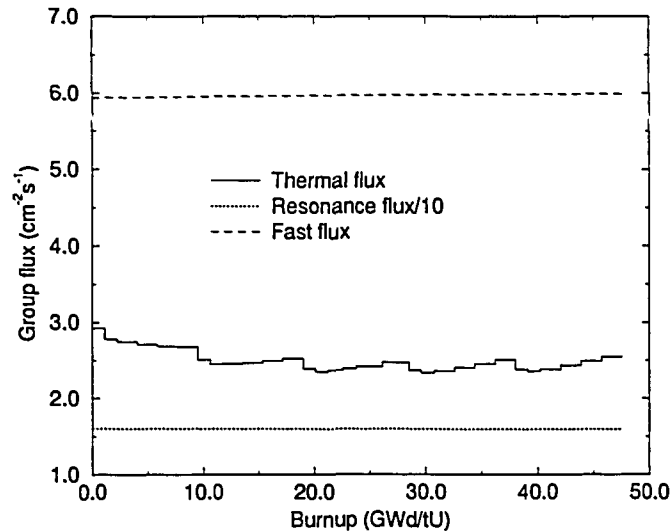


Figure 3.6 The thermal, resonance and fast neutron fluxes for the PWR-N4 as a function of burnup. All three fluxes are normalized to one fission neutron produced.

energy range in figure 3.8. The macroscopic cross section in the fast energy range is mainly determined by the fission cross section of ^{238}U , and has a constant value of about 0.01 cm^{-1} . From figure 3.7 can be seen that the resonance absorption cross section increases with about 15% from begin of life (BOL) to end of life (EOL). However, the absolute value of the resonance absorption rate is rather small (only about 20% of the neutrons are absorbed in the resonance energy range), so that an increase of the resonance absorption cross section with 15% will not have a large influence on the resonance flux (when the flux is normalized to one fission neutron produced, as is done in figure 3.6).

For the thermal energy range, this is different. A large fraction of the thermal neutrons will eventually be absorbed in the fuel, and when the absorption cross section in the thermal energy range increases, the thermal neutron flux decreases. The thermal neutron flux decreases during the first two burnup cycles (see figure 3.8), due to an increase of the thermal absorption cross section in the fuel, which is mainly caused by the buildup of ^{239}Pu , and to a lesser extend by the buildup of fission products. The increase of the thermal absorption cross section due to these two effects overcompensates the decrease of the thermal absorption cross section due to the depletion of ^{235}U . Only in the fourth and fifth burnup cycles, the depletion of ^{235}U leads to decreasing thermal absorption cross sections in the fuel region, and to a corresponding increase of the thermal neutron flux.

Thirdly, the RES and FAST values change also very much during each burnup cycle. This effect is also caused by changing macroscopic thermal cross sections, but now by the cross sections of the moderator. During each burnup cycle, the boron concentration in the moderator decreases from 1000 ppm at BOC to zero at EOC, which leads to a decrease of the thermal absorption cross section in the moderator, and a corresponding increase of the thermal neutron flux in the moderator and fuel regions.

Another effect which has an important influence on the resultant one-group cross sections, is the hardening of the fast neutron flux ($E > 1\text{ MeV}$) as a function of burnup (see figure 3.9). This is caused by the buildup of the two fissile plutonium

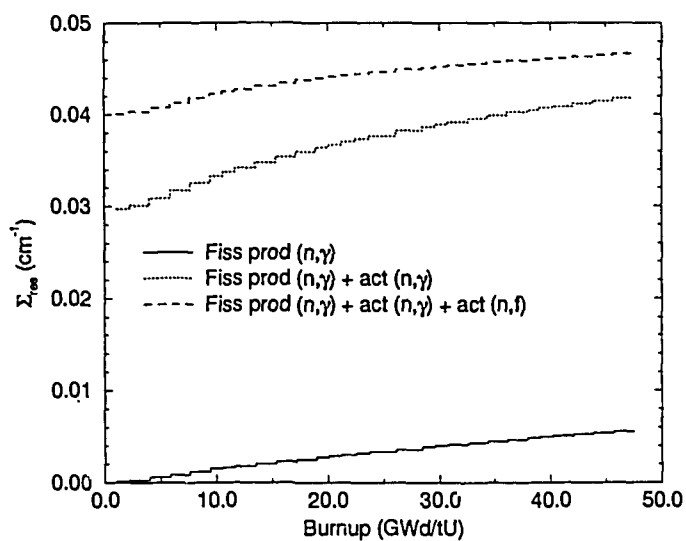


Figure 3.7 *Macroscopic resonance cross sections in the fuel of the PWR-N4 as a function of burnup.*

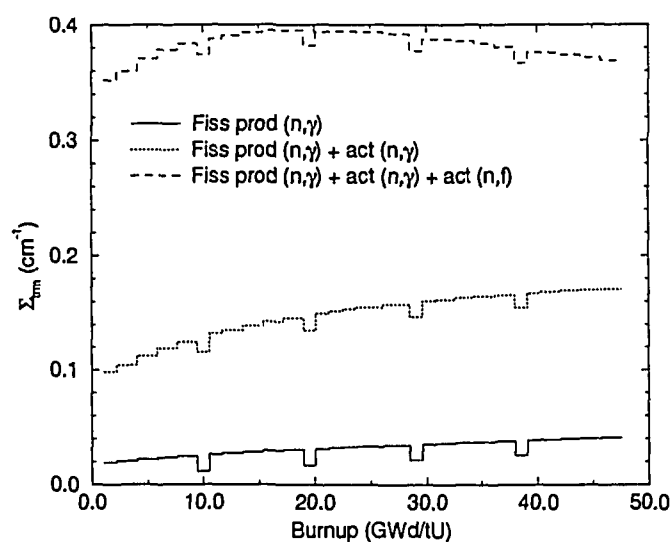


Figure 3.8 *Macroscopic thermal cross sections in the fuel of the PWR-N4 as a function of burnup.*

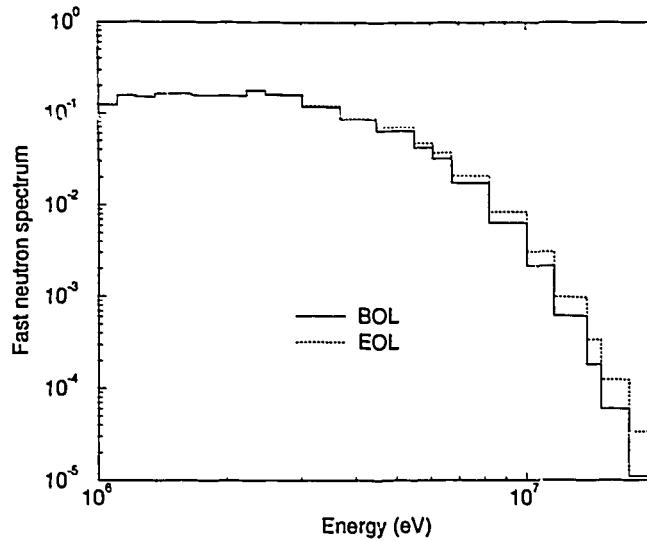


Figure 3.9 The spectrum of the fast neutron flux at BOL and at EOL for the PWR-N4. The fast neutron flux in both cases is normalized to unity.

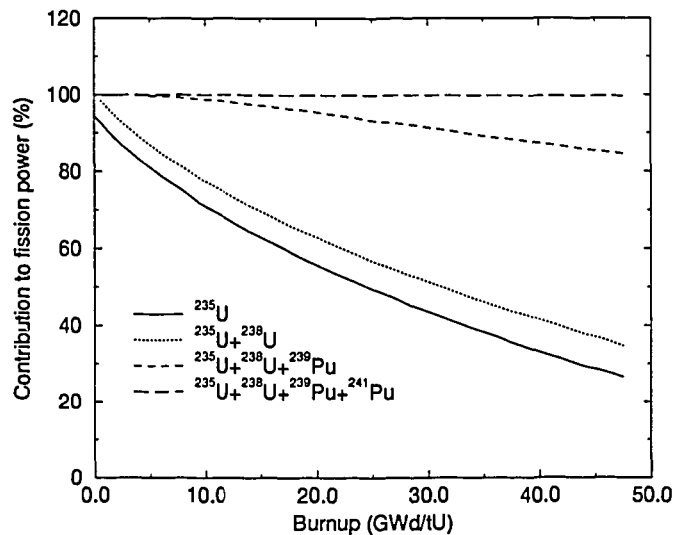


Figure 3.10 The contributions of the most important isotopes to the fission power density for the PWR-N4 as a function of burnup.

isotopes ^{239}Pu and ^{241}Pu . As can be seen in figure 3.10, the contribution of these two isotopes to the fission power density increases with burnup, and reaches nearly 50% at EOL for ^{239}Pu and about 15% at EOL for ^{241}Pu . Because the fission spectra of these two plutonium isotopes are (slightly) harder than the fission spectrum of ^{235}U , this leads to a continuous hardening of the fast neutron flux with increasing burnup. Although this spectrum hardening seems almost negligible, this effect is important for reactions with a threshold energy above 5 MeV, like (n,2n) and (n,3n) reactions.

All spectral effects described above, have their consequences for the one-group spectrum-averaged cross sections of the nuclides. The $1/\nu$ cross sections show an irregular behaviour as a function of burnup. This is illustrated in figure 3.11,

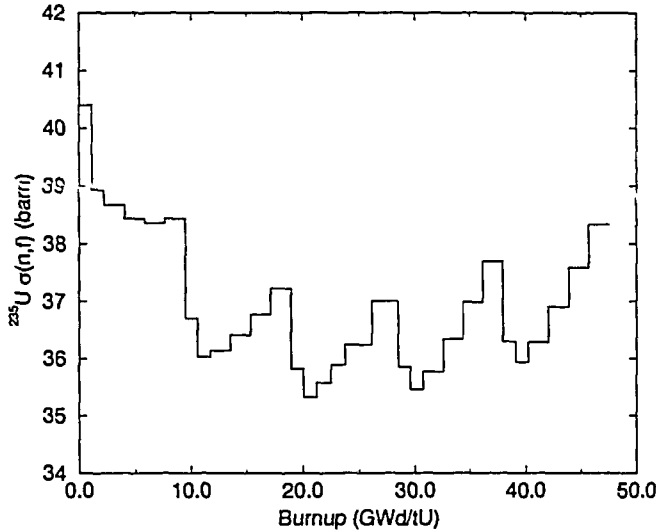


Figure 3.11 The microscopic (n,f) cross section of ^{235}U for the PWR-N4 as a function of burnup.

where the fission cross section of ^{235}U is shown as a function of burnup. The value of this cross section increases during each burnup cycle due to the decreasing boron concentration. Furthermore, there is a general tendency that $1/v$ cross sections decrease during the first two cycles, and increase again during the fourth and fifth cycles. This is due to the decrease of the thermal neutron flux relative to the resonance and fast neutron fluxes during the first two cycles, and the increase of the thermal neutron flux during the fourth and fifth cycles. This was explained before with figure 3.8. Because of the almost continuous hardening of the fast neutron spectrum, the high-threshold (n,2n) and (n,3n) cross sections show a smooth increase of several tens of percents as a function of burnup. This is seen in figure 3.12, where the (n,2n) cross section of ^{238}U is shown as a function of burnup.

3.2.3 Resultant cross sections

Each of the three-group ORIGEN-S cross sections is relatively independent of burnup as long as the cross-sectional changes are due to a changing resonance-to-thermal neutron flux ratio or to a changing fast-to-thermal neutron flux ratio. This is not the case, however, for high-threshold (n,2n) and (n,3n) cross sections and cross-sectional changes due to resonance shielding effects. The first two reaction types mainly depend on the neutron flux spectrum above 1 MeV; this spectrum shows a continuous hardening as a function of burnup, and the resonance integrals depend on the densities of the nuclides under consideration. The absorption resonance integral of ^{235}U , for example, increases from 235 barn at BOL to 251 barn at EOL, while the absorption resonance integral of ^{239}Pu decreases from 316 barn at BOL to 299 barn at EOL.

Table 3.3 gives the one-group (n, γ) cross sections of the actinides at BOL, average burnup (AVB), and EOL. The σ_{BU} values are the results of the fuel pin-cell calculations as described in section 3.1 (with regular cross-section updating during the burnup sequence), while the σ_{OR} cross sections are obtained by collapsing the new three-group ORIGEN-S cross sections to one group with the proper THERM,

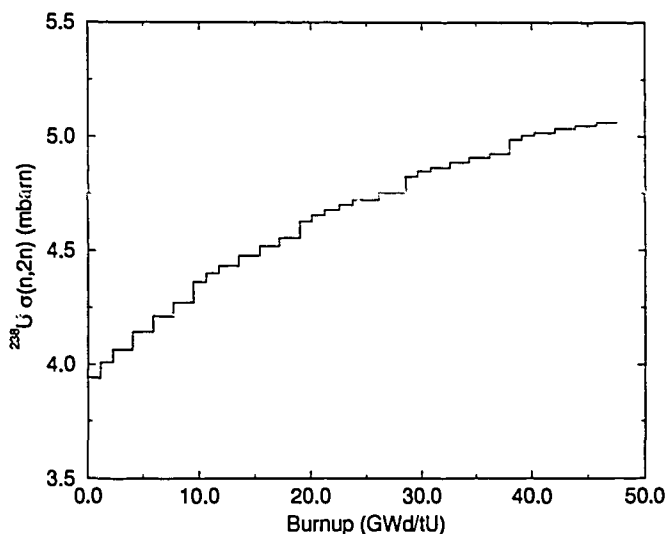


Figure 3.12 The microscopic (n,2n) cross section of ^{238}U for the PWR-N4 as a function of burnup.

RES and FAST values at BOL, AVB and EOL, respectively. This collapsing is done according to table 2.6. Note that at AVB, the σ_{BU} and σ_{OR} give exactly the same values because the three-group cross sections in the new ORIGEN-S libraries are calculated at AVB. It can be seen from table 3.3 that the σ_{OR} cross sections represent the σ_{BU} cross sections reasonably well, which is especially due to the fact that each of the three-group ORIGEN-S cross sections is not very dependent on burnup. A few exceptions are ^{236}U , ^{239}Pu and ^{240}Pu . For the first nuclide, it is the resonance integral which changes strongly as a function of burnup (the absorption resonance integral changes from 345 barn at BOL to 250 barn at EOL), while for the ^{239}Pu it is the strong resonance at 0.3 eV which causes the thermal cross section SIGNG (see table 2.5) to be very dependent on burnup. For ^{240}Pu it is the strong resonance at 1.0 eV which shows considerable self shielding with increasing nuclide density; the absorption resonance integral of ^{240}Pu decreases from 7352 barn at BOL to 2070 barn at EOL. These changes cannot be represented appropriately by the single-burnup cross sections used by ORIGEN-S, and it is therefore recommended to overwrite regularly the cross sections of these important nuclides during the burnup sequence.

The fission cross sections of the actinides at BOL, AVB and EOL are given in table 3.4. Again, a discrepancy of about 8% can be seen between the σ_{BU} and σ_{OR} cross sections for ^{239}Pu at BOL and at EOL. For all other nuclides, the differences between σ_{BU} and σ_{OR} are much smaller. This means that for the major part of the nuclides, the cross sections can well be represented by the three-group cross sections condensed to one group with proper THERM, RES and FAST values.

In table 3.5, the (n,2n) cross sections of the actinides at BOL, AVB and EOL are given. Because SIGN2N values are only given for the high-threshold (n,2n) cross sections (see table 2.6), cross-sectional changes which are only due to changing FAST values can be accounted for. This means that only cross-sectional changes due to changing ratios of fast-to-thermal neutron fluxes can be accounted for, while cross-sectional changes due to a changing spectral shape above 1 MeV are discarded. This can lead to rather large discrepancies at BOL and EOL, as can

Table 3.3 Comparison of one-group (n,γ) cross sections (barn) of the actinides for the PWR-N4 at BOL, AVB and EOL. The σ_{BU} cross sections are exact ones derived from the fuel pin cell calculations, the σ_{OR} cross sections are approximate ones obtained by collapsing the new three-group ORIGEN-S cross sections to one group with the proper THERM, RES and FAST values at BOL, AVB and EOL, respectively.

Nuclide	BOL		AVB	EOL	
	σ_{BU}	σ_{OR}	$\sigma_{BU/OR}$	σ_{BU}	σ_{OR}
²³⁴ U	21.55	20.69	20.14	20.34	20.69
²³⁵ U	8.960	9.006	8.279	9.013	8.946
²³⁶ U	8.586	6.712	6.791	6.146	6.745
²³⁸ U	0.916	0.927	0.918	0.939	0.929
²³⁷ Np	34.30	34.18	32.15	32.78	34.05
²³⁸ Np	14.28	14.22	12.64	14.05	14.07
²³⁹ Np	13.99	13.97	13.88	14.02	14.01
²³⁸ Pu	29.07	29.53	26.04	29.72	29.20
²³⁹ Pu	61.50	55.27	48.34	50.56	54.60
²⁴⁰ Pu	227.0	119.5	118.4	89.34	119.8
²⁴¹ Pu	37.32	35.43	31.18	33.90	35.03
²⁴² Pu	29.54	28.73	29.09	25.69	28.87
²⁴³ Pu	12.13	12.07	11.49	12.04	12.04
²⁴¹ Am	115.9	105.8	96.76	98.69	105.0
²⁴² Am	315.3	318.7	275.7	318.0	314.5
^{242m} Am	143.5	142.2	123.3	139.2	140.3
²⁴³ Am	52.21	50.04	50.17	48.01	50.23
²⁴² Cm	4.246	4.301	4.233	4.346	4.307
²⁴³ Cm	13.25	13.17	12.46	13.09	13.13
²⁴⁴ Cm	17.13	16.47	16.64	16.26	16.54
²⁴⁵ Cm	18.48	18.78	16.66	18.89	18.58
²⁴⁶ Cm	2.820	2.777	2.817	2.767	2.791

Table 3.4 Comparison of one-group (n,f) cross sections (barn) of the actinides for the PWK-N4 at BOL, AVB and EOL. The σ_{BU} cross sections are exact ones derived from the fuel pin cell calculations, the σ_{OR} cross sections are approximate ones obtained by collapsing the new three-group ORIGEN-S cross sections to one group with the proper THERM, RES and FAST values at BOL, AVB and EOL, respectively.

Nuclide	BOL		AVB	EOL	
	σ_{BU}	σ_{OR}	$\sigma_{BU/OR}$	σ_{BU}	σ_{OR}
²³⁴ U	0.522	0.522	0.531	0.530	0.530
²³⁵ U	40.40	40.34	35.89	40.00	39.93
²³⁶ U	0.312	0.291	0.297	0.288	0.295
²³⁸ U	0.102	0.102	0.105	0.105	0.104
²³⁷ Np	0.504	0.504	0.518	0.513	0.512
²³⁸ Np	140.6	139.7	124.1	138.3	138.2
²³⁹ Np	0.594	0.594	0.609	0.604	0.603
²³⁸ Pu	2.386	2.411	2.326	2.431	2.417
²³⁹ Pu	107.3	98.54	86.04	91.55	97.34
²⁴⁰ Pu	0.632	0.611	0.627	0.615	0.620
²⁴¹ Pu	109.9	105.5	93.02	101.5	104.3
²⁴² Pu	0.450	0.451	0.462	0.456	0.458
²⁴³ Pu	24.95	24.91	23.68	24.76	24.86
²⁴¹ Am	1.272	1.191	1.143	1.143	1.195
²⁴² Am	166.3	163.6	145.9	160.5	162.0
^{242m} Am	622.7	612.8	533.4	598.1	605.1
²⁴³ Am	0.428	0.426	0.438	0.433	0.434
²⁴² Cm	1.138	1.131	1.104	1.135	1.138
²⁴³ Cm		72.68	69.60		72.55
²⁴⁴ Cm	0.985	0.981	0.992	0.985	0.993
²⁴⁵ Cm		120.1	106.5		118.8
²⁴⁶ Cm	0.605	0.604	0.619	0.612	0.614

Table 3.5 *Comparison of one-group ($n,2n$) cross sections (mbarn) of the actinides for the PWR-N4 at BOL, AVB and EOL. The σ_{BU} cross sections are exact ones derived from the fuel pin cell calculations, the σ_{OR} cross sections are approximate ones obtained by collapsing the new three-group ORIGEN-S cross sections to one group with the proper THERM, RES and FAST values at BOL, AVB and EOL, respectively.*

Nuclide	BOL		AVB	EOL	
	σ_{BU}	σ_{OR}	$\sigma_{BU/OR}$	σ_{BU}	σ_{OR}
²³⁴ U	0.515	0.619	0.635	0.696	0.631
²³⁵ U	3.828	4.320	4.445	4.723	4.409
²³⁶ U	2.669	3.107	3.198	3.453	3.171
²³⁸ U	3.941	4.562	4.700	5.062	4.656
²³⁷ Np	0.791	0.947	0.975	1.068	0.966
²³⁸ Np	4.855	5.495	5.665	6.035	5.608
²³⁹ Np	1.195	1.379	1.419	1.525	1.407
²³⁸ Pu	0.263	0.316	0.325	0.357	0.322
²³⁹ Pu	1.064	1.234	1.270	1.369	1.259
²⁴⁰ Pu	1.064	1.510	1.553	1.682	1.541
²⁴¹ Pu	7.308	8.053	8.275	8.676	8.218
²⁴² Pu	2.179	2.533	2.607	2.812	2.585
²⁴³ Pu	17.28	18.87	19.42	20.28	19.26
²⁴¹ Am	0.601	0.712	0.734	0.800	0.727
²⁴² Am	1.422	1.607	1.653	1.757	1.640
^{242m} Am	3.888	4.389	4.515	4.797	4.479
²⁴³ Am	1.654	1.925	1.979	2.136	1.964
²⁴² Cm	0.359	0.439	0.452	0.492	0.448
²⁴³ Cm	1.214	1.389	1.430	1.522	1.418
²⁴⁴ Cm	1.507	1.780	1.831	1.973	1.816
²⁴⁵ Cm	1.346	1.552	1.597	1.705	1.584
²⁴⁶ Cm	1.650	1.963	2.020	2.206	2.004

be seen in table 3.5. Therefore, it is again recommended to overwrite the cross sections of the most important actinides during the burnup sequence.

3.3 Calculations and results on the LMFBR

3.3.1 Design data LMFBR

The French Superphénix reactor was used as a reference design for the burnup calculation on the LMFBR. Design data were kindly provided by CEA, and are tabulated in table 3.6.

3.3.2 Results

For the LMFBR, only one-group cross sections have been calculated according to the definitions in table 2.5. These definitions are used by ORIGEN-S as well as by other fuel depletion codes. Because the LMFBR cross sections do not vary much as a function of burnup (changes are usually less than 1%) the cross sections at AVB are sufficiently accurate, especially if it is taken into account that the Superphénix reactor was chosen as a characteristic example of a "typical" fast breeder reactor.

One-group cross sections at AVB are given in table 3.7 for the most important actinides.

Table 3.6 *Design data for the burnup calculations on the Superphénix reactor.*

Geometrical data (cm)	
Fuel outer radius	0.3715
Clad outer radius	0.3715
Lattice pitch	1.0947
Buckling height	108
Temperatures (K)	
Fuel ^{a)}	930
Coolant	743
Nuclide densities in the fuel/void at BOL (barn ⁻¹ cm ⁻¹)	
²³⁵ U	8.5188E-05
²³⁸ U	1.6091E-02
²³⁸ Pu	1.9953E-05
²³⁹ Pu	2.6926E-03
²⁴⁰ Pu	8.6867E-04
²⁴¹ Pu	1.8502E-04
²⁴² Pu	7.4018E-05
²⁴¹ Am	4.5022E-05
²³⁹ Pu	2.6926E-03
¹⁶ O	3.9734E-02
Nuclide densities in the clad/coolant (barn ⁻¹ cm ⁻¹)	
^{nat} Fe	2.3007E-02
^{nat} Cr	6.4570E-02
^{nat} Ni	4.7090E-02
^{nat} Si	3.8670E-04
⁵⁵ Mn	5.3920E-04
^{nat} Cu	1.0880E-04
^{nat} Ti	1.6490E-04
²³ Na	1.2660E-02
Burnup data	
Maximum burnup ^{b)} (MWd/tHM)	70000
Number of EFPD	640
Specific power (MWth/tHM)	109.375
Number of cell calculations in total	20
Number of actinides in cell	22
Number of fission products in cell	26

^{a)} This temperature is used for the calculations, although its value is rather low. A fuel temperature of 1500 K would have been more appropriate.

^{b)} Expected value for the first Superphenix core.

Table 3.7 *One-group cross sections of the actinides for the Superphénix reactor at AVB.*

Nuclide	σ_γ (barn)	σ_f (barn)	σ_{2n} (mbarn)
²³⁴ U	0.614	0.346	0.219
²³⁵ U	0.545	1.930	1.470
²³⁶ U	0.557	0.109	1.080
²³⁸ U	0.280	0.046	1.580
²³⁷ Np	1.580	0.334	0.335
²³⁸ Np	0.182	3.470	1.880
²³⁹ Np	1.970	0.473	0.476
²³⁸ Pu	0.557	1.130	0.112
²³⁹ Pu	0.522	1.830	0.428
²⁴⁰ Pu	0.561	0.397	0.527
²⁴¹ Pu	0.550	2.550	2.690
²⁴² Pu	0.489	0.275	0.880
²⁴³ Pu	0.391	0.865	6.300
²⁴¹ Am	1.940	0.278	0.251
^{242m} Am	0.486	3.190	1.490
²⁴² Am	0.608	3.210	0.546
²⁴³ Am	1.720	0.216	0.668
²⁴² Cm	0.532	0.596	0.155
²⁴³ Cm	0.227	3.270	0.473
²⁴⁴ Cm	0.587	0.444	0.617
²⁴⁵ Cm	0.332	2.720	0.530
²⁴⁶ Cm	0.243	0.281	0.692

4. UPDATE WITH EAF3 CROSS SECTIONS

4.1 Update of cross sections

Cross sections of nuclides which were not available from JEF2.2, have been updated in the ORIGEN-S libraries with cross sections from the EAF3 file (about 285 nuclides). The EAF3 file [7] is an extensive file containing point-wise activation cross sections for 729 target nuclides with atomic numbers ranging from 1 to 96 (Hydrogen to Curium). It also contains the activation cross sections for production of nuclides in a metastable state.

For the purpose of updating the cross sections in the ORIGEN-S libraries, the cross sections in the EAF3 file have been integrated to multi-group cross sections in XMAS group structure with an LWR spectrum used as a weighting function. The weighting function used for the integration procedure was equal to that used for the production of a JEF1.1 based cross-section library in XMAS group structure available at ECN. In this way, the multi-group cross sections from the EAF3 file for nuclides in the EAF3 which are known to be based on the JEF1.1 file, could be compared with cross sections from the JEF1.1 based cross-section library available at ECN, which has been thoroughly validated before. From this comparison was concluded that the integration procedure to calculate multi-group cross sections from the EAF3 file was done correctly.

After the integration of the EAF3 file to a multi-group cross-section library in XMAS structure, a three-group library was made for the LWR and a one-group library for the LMFBR by collapsing the multi-group library to three groups with the neutron spectrum of the PWR-N4 at average burnup, and to one group with the neutron spectra of Superphénix at average burnup. These spectra were the same as used for the collapsing of the JEF2.2 multi-group cross-section library to three groups for the LWR or to one group for the LMFBR, as explained in section 3.1. Finally these few-group cross sections were converted to ORIGEN-S format.

The whole procedure to update the cross sections in the ORIGEN-S data libraries with cross sections from the EAF3 file is schematically shown in figure 3.2 (the branch on the right hand side of that figure).

4.2 Update of isomer ratios

As mentioned before in sections 2.2 to 2.4, the three ASCII libraries contain the isomer ratio FNG1, and the light element library and actinide library contain also the isomer ratio FN2N1. The ratio FNG1 is used to describe the production of a product in a metastable state after an (n,γ) reaction, and the ratio FN2N1 is used to describe the production of a product in a metastable state after an $(n,2n)$ reaction. Both isomer ratios cannot be retrieved from the cross-section library based on the JEF2.2 file, which was used for the update of the cross sections as described in chapter 3, because this cross-section library does not contain these ratios. Because the EAF3 file does contain cross sections for the production of a nuclide in the ground state and in the first and second metastable states, the ratios FNG1 and FN2N1 can be retrieved from the EAF3 file. For this purpose, one-group cross sections for production of a nuclide in the ground state and in the first and second metastable states were calculated by collapsing the multi-group EAF3 library to one group by the neutron spectrum at AVB of the reactor under consideration (either the LWR or the LMFBR). Then, the ratios FNG1 and FN2N1

were calculated from these one-group cross sections according to the definitions given in tables 2.2 and 2.5.

Two assumptions have been made: first, the cross sections for both the production of a nuclide in the first metastable state and the second metastable state were summed to get the total cross section for production of a nuclide in "a" metastable state. This means that nuclides produced in the second metastable state are assumed to be in the first metastable state. The consequences of this assumption are most probably very small, because very few nuclides have data for production of nuclides in the second metastable state. Secondly, the calculated ratios are based on one-group cross sections for nuclides at infinite dilution, and it is assumed that these values are also valid for nuclides with considerable resonance shielding. Because many nuclides with ratios FNG1 or FN2N1 greater than zero will have low nuclide densities (and therefore negligible resonance shielding), this assumption will most probably not have large consequences.

However, there is one point of concern about the isomer ratio FNG1 calculated in this way. This ratio is determined in the EAF3 file at two energy points: at thermal energy (usually based on measurements), and at 14.5 MeV (usually adopted from systematics). The FN2N1 isomer ratio is usually calculated only at 14.5 MeV. A breakpoint energy is defined below which the thermal value is used and above which the fast value is used. When spectrum-averaged values for this ratio are to be calculated, the chosen value of the breakpoint energy has a large effect on the resultant values. This is illustrated with ^{241}Am , which is an important nuclide in this respect. The thermal value of FNG1 in the EAF3 file is 0.09, the value at 14.5 MeV is 0.5, and the breakpoint energy is 150 eV. Then, the spectrum-averaged FNG1 values for the PWR-N4 and Superphénix are 0.0995 and 0.4977, respectively. These values have to be compared with the original one in the old ORIGEN-S actinide library, which was 0.162 for both thermal and fast reactors. The new value for Superphénix is in contradiction with results from integral measurements in the Phénix reactor, which gives a spectrum-averaged FNG1 value of 0.15 [13]. For this reason, the FNG1 value for fast reactors has been changed in the new ORIGEN-S actinide library from 0.4977 to 0.15. For thermal reactors, the new FNG1 value of 0.0995 has not been changed, because no results on integral measurement in thermal reactors are known at this moment, and because it is clear from the measurements that the FNG1 value in thermal reactors should be lower than in fast reactors. In future versions of the EAF file, more accurate energy-dependent isomer ratios will be introduced with a smooth transition of this quantity from thermal to high energies.

5. VALIDATION OF THE NEW LIBRARIES

5.1 Calculations on the PWR-N4

Sample calculations on a fuel pin of the PWR-N4 have been performed to check the library. The burnup calculations for the PWR-N4, described in section 3.2, were repeated with the ORIGEN-S code using the new cross-section libraries. Note that in this case no intermediate pin-cell calculations were performed to calculate the neutron spectrum at several steps in the burnup sequence, but only the new cross-section data libraries with THERM, RES and FAST values at BOL and AVB, were used (0.518, 0.378 and 2.945 at BOL and 0.5335, 0.4613 and 3.625 at AVB, respectively).

Table 5.1 gives the actinide masses for the PWR-N4 at discharge burnup of 47.5 GWd/tU for both the burnup calculations with regular cross-section updating (according to picture C of figure 1.1 and figure 3.1) (subscript BU), and the burnup calculations using ORIGEN-S with the new cross-section libraries with proper values of THERM, RES and FAST at BOL and AVB (according to picture A of figure 1.1) (subscript OR).

From table 5.1, it is seen that the two ORIGEN-S burnup calculations with THERM, RES and FAST values of BOL and AVB give almost equal actinide masses at EOL. Generally, the $M_{OR,BOL}$ values are slightly lower than the $M_{OR,AVB}$ ones, because the (n,γ) and/or (n,f) cross sections of many actinides at BOL are higher than at AVB (see tables 3.3 and 3.4). This is especially so for ^{235}U , ^{237}Np , ^{239}Pu , ^{241}Pu , ^{241}Am and ^{242m}Am .

For most nuclides, the differences between the results of M_{BU} at the one side, and $M_{OR,BOL}$ and $M_{OR,AVB}$ at the other, are not much larger than the differences between the $M_{OR,BOL}$ and $M_{OR,AVB}$ results. Exceptions are ^{240}Np and ^{240m}Np . These are due to the isomer ratio FNG1 of ^{239}Np , which is zero in the old ORIGEN-S actinide library, and which has a value of 0.34 in the new one. This gives a much larger ^{240m}Np production when the new actinide library is used, and a reduced ^{240}Np production. Fortunately, both ^{240m}Np and ^{240}Np have small half lives of 65 and 7 minutes, respectively, which implies that after a few cooling days, the masses of both neptunium isotopes will effectively be zero.

Similar differences can be seen for ^{242m}Am and ^{242}Am , which are due to the isomer ratio FNG1 of ^{241}Am . For LWRs, the value of this parameter has changed from 0.162 in the old actinide library to 0.10 in the new one. This implies that the $^{241}\text{Am}(n,\gamma)^{242m}\text{Am}$ production is about 35% smaller when the new actinide library is used.

If capture cross sections which lead to nuclides in a metastable state are greater than zero, it must be checked whether data for such metastable nuclides are present in the cross-section libraries, as the daughter production of such metastable nuclides can otherwise seriously be underestimated. This is the case, for example, for ^{244m}Am . As both ^{244}Am and ^{244m}Am decay to ^{244}Cm and neither decay data nor cross-section data for ^{244m}Am are present in the current ORIGEN-S actinide libraries (neither in the old one, nor in the new one), the ^{244}Cm production is underestimated by about a factor of ten, in case that the $^{243}\text{Am}(n,\gamma)^{244m}\text{Am}$ cross section is not added to the $^{243}\text{Am}(n,\gamma)^{244}\text{Am}$ cross section.

5.2 Calculations on the burnup credit criticality benchmark

In 1992, a burnup credit criticality benchmark was specified, of which part I-B covers the prediction of the isotopic composition of PWR spent fuel. Physical data, operating history, specific power and nuclide densities at BOL were given for three different fuel samples with different burnup values of 27.35, 37.12 and 44.34 GWd/tU. For these samples, also measurements were done. All necessary data can be found in reference [14].

The calculations on these fuel samples can be divided in two parts. First, the proper THERM, RES and FAST values at BOL were calculated with the discrete-ordinates code XSDRNPM-S. Secondly, the burnup calculations with the ORIGEN-S code were performed using the three ASCII libraries. This means that the burnup calculations were done according to picture A of figure 1.1.

The results are given in tables 5.2, 5.3, and 5.4. It can be seen that for many nuclides, calculations with the new libraries give slightly better results than calculations with the old libraries. Discrepancies between the calculations and the measurements are generally within 10%, which seems quite good, because from table 5.1 follows that the discrepancies between burnup calculations with regular cross-section updating and burnup calculations with constant cross sections during the burnup sequence are of the same size. Large discrepancies can be seen in tables 5.2, 5.3, and 5.4 for the fission products ^{79}Se and ^{126}Sn . At this moment, the cause of these discrepancies is not clear.

It is noted that the results given in tables 5.2, 5.3, and 5.4 were obtained with data libraries where only the cross sections have been updated. However, results obtained with data libraries where also the fission product yields and decay data have been updated, are almost equal to those in the tables, except for ^{79}Se and ^{126}Sn . The large discrepancies for ^{79}Se are slightly reduced with about 10%, but the discrepancies for ^{126}Sn become even larger with almost 50%!

5.3 Calculations on Superphénix

Sample calculations on a fuel pin of Superphénix were performed to check the library for the fast reactor. The burnup calculations for Superphénix described in section 3.3, were repeated with the ORIGEN-S code using the new libraries. In this case no intermediate pin-cell calculations were performed to calculate the neutron spectrum at several steps in the burnup sequence, but only the new cross-section data libraries for the fast reactor were used.

Table 5.5 gives the masses of actinide isotopes for Superphénix at discharge burnup of 70 GWd/tHM for both the burnup calculations with regular cross section updating (according to picture C of figure 1.1 and figure 3.1) (subscript BU), and the burnup calculations using ORIGEN-S with the new cross-section data libraries for the fast reactor (according to picture A of figure 1.1) (subscript OR).

In general, the agreement between the two calculations is very good. This was expected, because it was found earlier that the cross sections for Superphénix do not change much as a function of burnup. The burnup calculations with regular cross-section updating should therefore give similar results to calculations where only the cross sections at AVB are used.

There are a few differences, however, which need some explanation. First, the

^{240}Np mass is underestimated in the M_{OR} results, due to the fact that in the new actinide library, the isomer ratio FNG1 of ^{239}Np has a value of 0.31 for the fast reactor, while that ratio is zero in the old libraries. This means that the $^{239}\text{Np}(n,\gamma)^{240}\text{Np}$ production is smaller with about 30% when the new actinide library is used. Again, it is noted that both ^{240}Np and ^{240m}Np have small half lives of 65 and 7 minutes, which implies that after a few cooling days the masses of both Np isotopes will effectively be zero.

Secondly, the ^{242m}Am mass is smaller in the M_{OR} results with about 7%. For fast reactors, the isomer ratio FNG1 of ^{241}Am has changed from 0.162 in the old actinide library to 0.15 in the new one, which implies that the $^{241}\text{Am}(n,\gamma)^{242m}\text{Am}$ production is about 7% smaller when the new actinide library is used.

Thirdly, there are some large discrepancies for the curium isotopes. These are mainly due to the fact that the cross sections of the curium isotopes are different for the M_{BU} results and the M_{OR} ones. The cross sections of the curium isotopes were reprocessed during the project because some large discrepancies were found between the fast-reactor one-group cross sections of these isotopes calculated at CEA and at ECN. For example, the capture and fission cross sections of ^{245}Cm decreased by more than a factor of two after the recalculation of these cross sections, which lead to higher masses for ^{245}Cm in the M_{OR} results, and to lower masses for ^{246}Cm . The M_{OR} are expected to be more accurate.

Table 5.1 Nuclide masses and differences at EOL (47.5 GWd/tU) per initial ton uranium for the PWR-N4 from the burnup calculations with regular cross-section updating (M_{BU}), and from ORIGIN-S calculations with the new libraries with proper THERM, RES and FAST values at BOL ($M_{OR,BOL}$) and AVB ($M_{OR,AVB}$).

Nuclide	M_{BU}	$M_{OR,BOL}$		$M_{OR,AVB}$	
	(g)	(g)	diff (%)	(g)	diff (%)
^{234}U	1.55E+02	1.58E+02	1.9	1.56E+02	0.6
^{235}U	7.78E+03	7.31E+03	-6.0	8.03E+03	3.2
^{236}U	5.17E+03	5.17E+03	0.0	5.15E+03	-0.4
^{237}U	1.15E+01	1.21E+01	5.2	1.24E+01	7.8
^{238}U	9.24E+05	9.26E+05	0.2	9.24E+05	0.0
^{239}U	6.60E-01	6.52E-01	-1.2	6.54E-01	-0.9
^{237}Np	6.35E+02	6.11E+02	-3.8	6.49E+02	2.2
^{238}Np	2.00	2.04	2.0	2.07	3.5
^{239}Np	9.47E+01	9.39E+01	-0.8	9.43E+01	-0.4
^{240}Np	2.81E-03	1.84E-03	-34.5	1.86E-03	-33.8
^{240m}Np	8.93E-23	1.05E-04	.	1.07E-04	.
^{238}Pu	2.89E+02	2.77E+02	-4.2	2.97E+02	2.8
^{239}Pu	6.41E+03	5.64E+03	-12.0	6.36E+03	-0.8
^{240}Pu	2.95E+03	2.50E+03	-15.3	2.49E+03	-15.6
^{241}Pu	1.78E+03	1.86E+03	4.5	2.05E+03	15.2
^{242}Pu	7.98E+02	8.53E+02	6.9	8.44E+02	5.8
^{243}Pu	2.01E-01	2.36E-01	17.4	2.40E-01	19.4
^{241}Am	7.06E+01	6.96E+01	-1.4	8.03E+01	13.7
^{242}Am	1.76E-01	2.04E-01	15.9	2.19E-01	24.4
^{242m}Am	1.59	9.72E-01	-38.9	1.17	-26.4
^{243}Am	1.83E+02	1.93E+02	5.5	1.99E+02	8.7
^{244}Am	1.73E-01	1.89E-01	9.2	1.98E-01	14.5
^{242}Cm	2.64E+01	2.99E+01	13.3	3.20E+01	21.2
^{243}Cm	7.30E-01	7.64E-01	4.7	8.32E-01	14.0
^{244}Cm	7.55E+01	7.18E+01	-4.9	7.76E+01	2.8
^{245}Cm	4.97	4.35	-12.5	5.22	5.0
^{246}Cm	5.48E-01	4.73E-01	-13.7	5.19E-01	-5.3

Table 5.2 Nuclide concentrations at a burnup of 27.35 GWdtU (mg/g UO_2 and mCi/g UO_2 (*)) for the Burnup Credit Criticality Benchmark part I-B. THERM, RES and FAST are 0.54, 0.25 and 2.00, respectively.

Nuclide	Measurements value	New Library value	C/E	Old Library value	C/E
^{234}U	1.6E-01	1.61E-01	1.01	1.33E-01	0.83
^{235}U	8.47	8.00	0.94	8.08	0.95
^{236}U	3.14	3.13	1.00	3.54	1.13
^{238}U	8.425E+02	8.38E+02	0.99	8.37E+02	0.99
^{238}Pu	1.012E-01	7.80E-02	0.77	9.78E-02	0.97
^{239}Pu	4.264	3.66	0.86	4.22	0.99
^{240}Pu	1.719	1.86	1.08	1.69	0.98
^{241}Pu	6.812E-01	6.72E-01	0.99	5.31E-01	0.78
^{242}Pu	2.886E-01	2.80E-02	0.97	2.00E-02	0.69
^{237}Np *	1.89E-04	1.60E-04	0.85	2.26E-04	1.20
^{241}Am *	8.56E-01	7.97E-01	0.93	6.05E-01	0.71
^{79}Se *	4.55E-05	2.75E-04	6.04	2.79E-04	6.13
^{90}Sr *	4.59E+01	4.93E+01	1.07	4.83E+01	1.05
^{99}Tc *	9.59E-03	1.03E-02	1.07	1.05E-02	1.09
^{126}Sn *	1.25E-04	3.85E-04	3.08	3.97E-04	3.18
^{135}Cs *	4.16E-04	4.28E-04	1.03	3.93E-04	0.94
^{137}Cs *	6.71E+01	6.80E+01	1.01	6.77E+01	1.01

Table 5.3 Nuclide concentrations at a burnup of 37.12 GWdtU (mg/g UO_2 and mCi/g UO_2 (*)) for the Burnup Credit Criticality Benchmark part I-B. THERM, RES and FAST are 0.54, 0.25 and 2.00, respectively.

Nuclide	Measurements value	New Library value	C/E	Old Library value	C/E
^{234}U	1.4E-01	1.39E-01	0.99	1.08E-01	0.77
^{235}U	5.17	4.68	0.91	4.83	0.93
^{236}U	3.53	3.53	1.00	3.93	1.11
^{238}U	8.327E+02	8.31E+02	1.00	8.30E+02	1.00
^{238}Pu	1.893E-01	1.58E-01	0.83	1.96E-01	1.04
^{239}Pu	4.357	3.71	0.85	4.31	0.99
^{240}Pu	2.239	2.17	0.97	2.04	0.91
^{241}Pu	9.028E-01	9.21E-01	1.02	7.51E-01	0.83
^{242}Pu	5.761E-01	6.10E-01	1.06	4.20E-01	0.73
^{237}Np *	2.51E-04	2.38E-04	0.95	3.34E-04	1.33
^{241}Am *	1.18	1.07	0.91	8.38E-01	0.71
^{79}Se *	6.036E-05	3.66E-04	6.06	3.73E-04	6.18
^{90}Sr *	5.9E+01	6.20E+01	1.05	6.07E+01	1.03
^{99}Tc *	1.23E-02	1.35E-02	1.10	1.39E-02	1.13
^{126}Sn *	1.82E-04	5.72E-04	3.14	5.88E-04	3.23
^{135}Cs *	4.59E-04	4.63E-04	1.01	4.25E-04	0.93
^{137}Cs *	9.01E+01	9.20E+01	1.02	9.16E+01	1.02

Table 5.4 Nuclide concentrations at a burnup of 44.34 GWd/tU (mg/g UO_2 and mCi/g UO_2 (*)) for the Burnup Credit Criticality Benchmark part I-B. THERM, RES and FAST are 0.54, 0.25 and 2.00, respectively.

Nuclide	Measurements	New Library		Old Library	
	value	value	C/E	value	C/E
^{234}U	1.2E-01	1.24E-01	1.03	9.03E-02	0.78
^{235}U	3.54	3.04	0.86	3.20	0.90
^{236}U	3.69	3.65	0.99	4.03	1.09
^{238}U	8.249E+02	8.25E+02	1.00	8.24E+02	1.00
^{238}Pu	2.688E-01	2.27E-01	0.84	2.81E-01	1.05
^{239}Pu	4.357	3.71	0.85	4.32	0.99
^{240}Pu	2.543	2.28	0.90	2.18	0.86
^{241}Pu	1.020	1.03	1.01	8.56E-01	0.84
^{242}Pu	8.401E-01	8.90E-01	1.06	5.96E-01	0.71
^{237}Np *	3.31E-04	2.91E-04	0.88	4.05E-04	1.22
^{241}Am *	1.31	1.17	0.89	9.38E-01	0.72
^{79}Se *	6.49E-05	4.30E-04	6.63	4.41E-04	6.80
^{90}Sr *	6.58E+01	7.01E+01	1.07	6.87E+01	1.04
^{99}Tc *	1.35E-02	1.56E-02	1.16	1.62E-02	1.20
^{126}Sn *	2.2E-04	7.22E-04	3.28	7.40E-04	3.36
^{135}Cs *	4.95E-04	4.83E-04	0.98	4.43E-04	0.89
^{137}Cs *	1.09E+02	1.10E+02	1.01	1.09E+02	1.00

Table 5.5 *Actinide masses and differences at EOL (70 GWd/tHM) per initial ton of fuel for the Superphénix reactor from the burnup calculations with regular cross-section updating (M_{BU}), and from ORIGEN-S calculations with the new libraries (M_{OR}).*

Nuclide	M_{BU} (g)	M_{OR} (g)	diff (%)
^{234}U	1.13E+01	1.14E+01	0.9
^{235}U	1.93E+03	1.92E+03	-0.5
^{236}U	3.66E+02	3.66E+02	0.0
^{237}U	5.14	5.22	1.6
^{238}U	6.49E+05	6.48E+05	-0.2
^{239}U	1.91	1.89	-1.0
^{237}Np	2.45E+02	2.46E+02	-0.4
^{238}Np	5.21E-01	5.20E-01	-0.2
^{239}Np	2.73E+02	2.71E+02	-0.7
^{240m}Np	1.62E-06	5.44E-04	.
^{240}Np	1.56E-02	1.06E-02	-32.1
^{238}Pu	9.27E+02	9.40E+02	1.4
^{239}Pu	1.01E+05	1.01E+05	0.0
^{240}Pu	4.33E+04	4.33E+04	0.0
^{241}Pu	7.42E+03	7.41E+03	-0.1
^{242}Pu	3.84E+03	3.84E+03	0.0
^{243}Pu	2.49E-01	2.47E-01	-0.8
^{241}Am	1.59E+03	1.60E+03	0.6
^{242m}Am	9.34E+01	8.67E+01	-7.2
^{242}Am	1.10	1.12	1.8
^{243}Am	3.73E+02	3.73E+02	0.0
^{244}Am	1.73E-01	1.72E-01	-0.6
^{242}Cm	1.91E+02	1.99E+02	4.2
^{243}Cm	1.69E+01	1.48E+01	-12.4
^{244}Cm	8.22E+01	8.03E+01	-2.3
^{245}Cm	2.95	3.62	22.7
^{246}Cm	1.71E-01	8.33E-02	-51.3

6. CONCLUSIONS

Cross-section data libraries for the ORIGEN-S fuel depletion code have been updated with cross sections from the JEF2.2 evaluated nuclear data file and the EAF3 activation file. For both an LWR and a LMFBR, cross sections of 517 light elements, 65 actinides and 319 fission products have been renewed or added to the libraries (in total cross sections of 604 different nuclides). Also isomer ratios for both reactor types have been updated based on the EAF3 file.

For the LWR, the French PWR-N4 reactor was used as a reference design. Cross sections of this reactor type vary considerably as a function of burnup. In general, cross sections with a $1/v$ energy dependence tend to decrease during the first two cycles, and to increase again during the last two cycles (of 9.5 MWd/tU each). This is because the thermal neutron flux first decreases due to increasing macroscopic absorption cross sections in the thermal energy range (due to buildup of plutonium isotopes and fission products), and then increases again due to decreasing absorption cross sections (due to depletion of ^{235}U).

In contradiction to this behaviour, $(n,2n)$ and other threshold reactions show a smooth increase with burnup with several tens of percents. This is due to the increasing importance of plutonium isotopes with respect to the fission rate, and because ^{239}Pu and ^{241}Pu have slightly harder fission spectra compared to ^{235}U .

For the LMFBR, the Superphénix reactor was used as a reference design. Also for this reactor the cross sections have been calculated as a function of burnup, but the variation turned out to be very small.

The new cross-section data libraries have been validated by comparing results of calculations with regular cross-section updates during the burnup sequence and without these updates. The agreement between the two groups of results is satisfactory, and some discrepancies could be explained. In general, it is concluded from these calculations that regular updates of the cross sections during the burnup sequence remain necessary for the most important actinides and fission products (say 10 to 20) in order to account for the burnup dependence of the cross sections of these nuclides. This is especially so for the LWR. For all other nuclides (the bulk of the nuclides), the cross sections in the new ORIGEN-S libraries can be used without making large errors.

Calculations have also been done on the burnup credit criticality benchmark. The results of these benchmark calculations agree well with the measurements, except for the activity of the fission products ^{79}Se and ^{126}Sn . The reasons for these discrepancies are not clear yet.

7. ACKNOWLEDGEMENTS

The author acknowledges the Commission of the European Union for co-funding this work under contract number F12W-CT-91-0104, and CEA for providing the data for the PWR-N4 reactor and the fast reactor Superphénix.

REFERENCES

- [1] O.W. Hermann and R.M. Westfall. *ORIGEN-S, SCALE Module to Calculate Fuel Depletion, Actinide Transmutation, Fission Product Buildup and Decay, and Associated Radiation Source Terms*. Oak Ridge National Laboratory, Oak Ridge, Tennessee, USA, Feb 1989.
- [2] J.L. Kloosterman. *New Working Libraries for Transmutation Studies*. In GLOBAL'93, Seattle, Washington, USA, pages 1229–1236, Sep 1993.
- [3] J.E. Hoogenboom and J.L. Kloosterman. *Production and Validation of ORIGEN-S libraries from JEF2.2 and EAF3 data*. Technical report, Interfaculty Reactor Institute, Delft University of Technology, To be published 1995.
- [4] J.C. Ryman. *ORIGEN-S Data Libraries*. Oak Ridge National Laboratory, Oak Ridge, Tennessee, USA, Feb 1983.
- [5] O.W. Hermann. *COUPLE-S, SCALE Module to Process Problem-Dependent Cross Sections and Neutron Spectral Data for ORIGEN-S Analysis*. Oak Ridge National Laboratory, Oak Ridge, Tennessee, USA, Oct 1981.
- [6] ICRP. *Annual Limits on Intake of Radionuclides by Workers Based on the 1990 Recommendations*. Technical Report Publication 61, ICRP, 1990.
- [7] J. Kopecky *et al.* *The European Activation File EAF3 with Neutron Activation and Transmutation Cross Sections*. Technical Report ECN-C-92-058, Netherlands Energy Research Foundation (ECN), Petten, The Netherlands, Sep 1992.
- [8] D.W. Muir R.E. MacFarlane and R.M. Boicourt. *NJOY87, A Code System for Producing Pointwise and Multigroup Neutron and Photon Cross Sections from ENDF/B Evaluated Nuclear Data*. Technical Report PSR-171, Los Alamos National Laboratory, Los Alamos, New Mexico, USA, 1987.
- [9] N.M. Greene. *BONAMI-S, Resonance Self-Shielding by the Bondarenko Method*. Oak Ridge National Laboratory, Oak Ridge, Tennessee, USA, Aug 1981.
- [10] L.M. Petrie N.M. Greene and R.M. Westfall. *NITAWL-II, SCALE Module for Performing Resonance Shielding and Working Library Production*. Oak Ridge National Laboratory, Oak Ridge, Tennessee, USA, Jun 1989.
- [11] N.M. Greene and L.M. Petrie. *XSDRNPM-S, A One-Dimensional Discrete-Ordinates Code for Transport Analysis*. Oak Ridge National Laboratory, Oak Ridge, Tennessee, USA, Jan 1983.
- [12] G. Abu-Zaied *et al.* *Impact of Boron History on Physics Parameters of PWR Fuel Assemblies*. In PHYSOR'90, Marseille, France, pages XIV12–XIV19, Apr 1990.
- [13] A. D'Angelo *et al.* *Analysis of Sample and Fuel Pin Irradiation Experiments in Phenix for Basic Nuclear Data Validation*. Nuclear Science and Engineering, 105:244–255, 1990.
- [14] M.C. Brady. *Burnup Credit Criticality Benchmark, Part I-B, Isotopic Prediction*. Technical Report NEA/NSC/DOC(92)10/REV, Nuclear Energy Agency, Nov 1992.

APPENDIX A. LIST OF SYMBOLS

Table A.1 *List of symbols and abbreviations used in this report.*

Symbol	Unit	Description
AVB		Average Burnup
BOC		Begin Of Cycle
BOL		Begin Of Life
EFPD		Effective Full Power Day
EOC		End Of Cycle
EOL		End Of Life
E_0	eV	Thermal energy 0.0253 eV.
I	barn	Resonance integral $\int_{0.5}^{10^6} \frac{\sigma_a(E)}{E} dE$.
σ_0	barn	Cross section at thermal energy E_0 .
σ_1	barn	Cross section averaged over fission spectrum.
$\phi(E)$	$\text{cm}^{-2}\text{s}^{-1}\text{eV}^{-1}$	Neutron flux.
ϕ_{thm}	$\text{cm}^{-2}\text{s}^{-1}$	Thermal neutron flux ($E < 0.5$).
ϕ_{res}	$\text{cm}^{-2}\text{s}^{-1}$	Resonance neutron flux ($0.5 < E < 10^6$).
ϕ_{fst}	$\text{cm}^{-2}\text{s}^{-1}$	Fast neutron flux ($E > 10^6$).
ϕ_{fis}	$\text{cm}^{-2}\text{s}^{-1}$	Fission spectrum.
$\sigma_a(E)$	cm^{-2}	Microscopic absorption cross section as a function of energy. (sum of $\sigma_\gamma(E)$, $\sigma_f(E)$, $\sigma_\alpha(E)$ and $\sigma_p(E)$)
σ_a	cm^{-2}	Microscopic one-group absorption cross section.
$\sigma_f(E)$	cm^{-2}	Microscopic fission cross section as a function of energy.
σ_f	cm^{-2}	Microscopic one-group fission cross section.
$\sigma_\gamma(E)$	cm^{-2}	Microscopic (n, γ) cross section as a function of energy.
σ_γ	cm^{-2}	Microscopic one-group (n, γ) cross section.
$\sigma_\gamma^1(E)$	cm^{-2}	Microscopic (n, γ) cross section for production of a nuclide in the first metastable state as a function of energy.
$\sigma_\gamma^2(E)$	cm^{-2}	Microscopic (n, γ) cross section for production of a nuclide in the second metastable state as a function of energy.
$\sigma_\alpha(E)$	cm^{-2}	Microscopic (n, α) cross section as a function of energy.
σ_α	cm^{-2}	Microscopic one-group (n, α) cross section as a function of energy.
$\sigma_p(E)$	cm^{-2}	Microscopic (n,p) cross section as a function of energy.
σ_p	cm^{-2}	Microscopic one-group (n,p) cross section.
$\sigma_{2n}(E)$	cm^{-2}	Microscopic (n,2n) cross section as a function of energy.
σ_{2n}	cm^{-2}	Microscopic one-group (n,2n) cross section.
$\sigma_{2n}^1(E)$	cm^{-2}	Microscopic (n,2n) cross section for production of a nuclide in the first metastable state as a function of energy.
σ_{2n}^1	cm^{-2}	Microscopic one-group (n,2n) cross section for production of a nuclide in the first metastable state.
$\sigma_{2n}^2(E)$	cm^{-2}	Microscopic (n,2n) cross section for production of a nuclide in the second metastable state as a function of energy.
σ_{2n}^2	cm^{-2}	Microscopic one-group (n,2n) cross section for production of a nuclide in the second metastable state.
T	K	Temperature.
T_0	K	Room temperature 293.6 K.

APPENDIX B. ORIGIN OF CROSS SECTIONS

The following three tables give the origin of the cross sections in the three different libraries. This is only done for the nuclides for which cross sections have been updated. Nuclides for which only the decay-data record has been updated, and for which no new cross sections were available are not listed in these tables. Also nuclides for which neither the decay-data record, nor the cross-section records have been updated, are listed in these tables. The total number of nuclides in the three different libraries is therefore greater than the number of nuclides listed in these tables.

The notation for the nuclides in column two of the following tables is given as $Z \cdot 10000 + A \cdot 10 + M$, where Z is the atomic number of the nuclide, A is the atomic mass, and M is the metastable state of the nuclide ($M = 0$ means the nuclide in the ground state, $M = 1$ means the nuclide in the first metastable state, etc.).

The third and fourth columns indicate whether the new cross sections are based on JEF2.2 data or on EAF3 data. For each line, the items in these two columns sum to 2, because for each nuclide, the cross sections have been updated for two reactor types (both an LWR and a LMFBR).

The fifth and sixth columns ("Cell calculations") indicate whether the specific nuclide was included in the cell calculations or not. If so, the cross sections of that nuclide at AVB obtained from the cell calculations have been used to update the ORIGEN-S libraries.

In general, the origin of the cross sections for a specific nuclide is equal for both reactor types, but the treatment of the data may be different for the LWR and the LMFBR. For example, the number of fission products explicitly accounted for in the fuel pin cell calculations is different for the LWR and the LMFBR (see table 3.1). This can then be seen in the fifth and sixth columns under the heading "Cell calculation". Furthermore, it is noted that not only the cross sections from the nuclides in the fuel zone in the pin cell calculations are used for the update, but also the cross sections from the nuclides in the cladding/structural and moderator/coolant zones. The number of nuclides with cross sections from the cell calculations is therefore greater than the number of actinides and fission products given in table 3.1.

The seventh column, finally, indicates whether the data for a specific nuclide were added to the library or not. If so, the number in this column equals 2, because cross-section data have always been added for both the LWR and the LMFBR.

Table B.1 *Origin of cross sections in the light element library.*

Number	Nuclide	JEF2.2	EAF3	Cell calculation		Added
				PWR	LMFBR	
1	10010	2	0	1	0	0
2	10020	2	0	0	0	0
3	10030	0	2	0	0	0
4	20030	2	0	0	0	0
5	30060	2	0	0	0	0
6	30070	2	0	0	0	0
7	40090	2	0	0	0	0
8	40100	0	2	0	0	0
9	50100	2	0	1	0	0
10	50110	2	0	1	0	0
11	60120	0	2	0	0	0
12	60130	0	2	0	0	0
13	60140	0	2	0	0	0
14	70140	2	0	0	0	0
15	70150	2	0	0	0	0
16	80160	2	0	1	1	0
17	80170	0	2	0	0	0
18	80180	0	2	0	0	0
19	90190	2	0	0	0	0
20	100200	0	2	0	0	0
21	100210	0	2	0	0	0
22	100220	0	2	0	0	0
23	110220	0	2	0	0	0
24	110230	2	0	0	1	0
25	110240	0	2	0	0	0
26	120240	0	2	0	0	0
27	120250	0	2	0	0	0
28	120260	0	2	0	0	0
29	120280	0	2	0	0	0
30	130270	2	0	0	0	0
31	140280	0	2	0	0	0
32	140290	0	2	0	0	0
33	140300	0	2	0	0	0
34	140310	0	2	0	0	0
35	140320	0	2	0	0	0
36	150310	0	2	0	0	0
37	150320	0	2	0	0	0
38	150330	0	2	0	0	0
39	160320	2	0	0	0	0
40	160330	2	0	0	0	0

Table B.1 *Table continued.*

Number	Nuclide	JEF2.2	EAF3	Cell calculation		Added
				PWR	LMFBR	
41	160340	2	0	0	0	0
42	160350	0	2	0	0	0
43	160360	2	0	0	0	0
44	170350	0	2	0	0	0
45	170360	0	2	0	0	0
46	170370	0	2	0	0	0
47	180360	0	2	0	0	0
48	180370	0	2	0	0	0
49	180380	0	2	0	0	0
50	180390	0	2	0	0	0
51	180400	0	2	0	0	0
52	180410	0	2	0	0	0
53	180420	0	2	0	0	0
54	190390	0	2	0	0	0
55	190400	0	2	0	0	0
56	190410	0	2	0	0	0
57	190420	0	2	0	0	0
58	190430	0	2	0	0	0
59	200400	0	2	0	0	0
60	200410	0	2	0	0	0
61	200420	0	2	0	0	0
62	200430	0	2	0	0	0
63	200440	0	2	0	0	0
64	200450	0	2	0	0	0
65	200460	0	2	0	0	0
66	200470	0	2	0	0	0
67	200480	0	2	0	0	0
68	210441	0	2	0	0	2
69	210450	0	2	0	0	0
70	210460	0	2	0	0	0
71	210470	0	2	0	0	0
72	210480	0	2	0	0	0
73	220460	0	2	0	0	0
74	220470	0	2	0	0	0
75	220480	0	2	0	0	0
76	220490	0	2	0	0	0
77	220500	0	2	0	0	0
78	230490	0	2	0	0	0
79	230500	0	2	0	0	0
80	230510	0	2	0	0	0

Table B.1 *Table continued.*

Number	Nuclide	JEF2.2	EAF3	Cell calculation		Added
				PWR	LMFBR	
81	240500	2	0	1	1	0
82	240510	0	2	0	0	0
83	240520	2	0	1	1	0
84	240530	2	0	1	1	0
85	240540	2	0	1	1	0
86	250540	0	2	0	0	0
87	250550	1	1	0	1	0
88	260540	2	0	1	1	0
89	260550	0	2	0	0	0
90	260560	2	0	1	1	0
91	260570	2	0	1	1	0
92	260580	2	0	1	1	0
93	260590	0	2	0	0	0
94	270580	0	2	0	0	0
95	270590	2	0	0	0	0
96	270600	0	2	0	0	0
97	280580	2	0	0	1	0
98	280590	0	2	0	0	0
99	280600	2	0	0	1	0
100	280610	2	0	0	1	0
101	280620	2	0	0	1	0
102	280630	0	2	0	0	0
103	280640	2	0	0	1	0
104	280660	0	2	0	0	0
105	290630	0	2	0	0	0
106	290640	0	2	0	0	0
107	290650	0	2	0	0	0
108	290670	0	2	0	0	0
109	300640	0	2	0	0	0
110	300650	0	2	0	0	0
111	300660	0	2	0	0	0
112	300670	0	2	0	0	0
113	300680	0	2	0	0	0
114	300691	0	2	0	0	0
115	300700	0	2	0	0	0
116	310690	0	2	0	0	0
117	310710	0	2	0	0	0
118	310720	0	2	0	0	0
119	320700	0	2	0	0	0
120	320710	0	2	0	0	0

Table B.1 *Table continued.*

Number	Nuclide	JEF2.2	EAF3	Cell calculation		Added
				PWR	LMFBR	
121	320720	2	0	0	0	0
122	320730	2	0	0	0	0
123	320740	2	0	0	0	0
124	320760	0	2	0	0	0
125	320770	0	2	0	0	0
126	330750	2	0	0	0	0
127	330760	0	2	0	0	0
128	330770	0	2	0	0	0
129	340740	2	0	0	0	0
130	340750	0	2	0	0	0
131	340760	2	0	0	0	0
132	340770	2	0	0	0	0
133	340780	2	0	0	0	0
134	340790	0	2	0	0	0
135	340800	2	0	0	0	0
136	340820	2	0	0	0	0
137	350790	2	0	0	0	0
138	350810	2	0	0	0	0
139	350820	0	2	0	0	0
140	360780	2	0	0	0	0
141	360790	0	2	0	0	0
142	360800	2	0	0	0	0
143	360810	0	2	0	0	0
144	360820	2	0	0	0	0
145	360830	2	0	1	0	0
146	360840	2	0	0	0	0
147	360850	2	0	0	0	0
148	360860	2	0	0	0	0
149	370850	2	0	0	0	0
150	370860	2	0	0	0	0
151	370870	2	0	0	0	0
152	380840	2	0	0	0	0
153	380850	0	2	0	0	0
154	380860	2	0	0	0	0
155	380870	2	0	0	0	0
156	380880	2	0	0	0	0
157	380890	2	0	0	0	0
158	380900	2	0	0	0	0
159	390890	2	0	0	0	0
160	390900	2	0	0	0	0

Table B.1 *Table continued.*

Number	Nuclide	JEF2.2	EAF3	Cell calculation		Added
				PWR	LMFBR	
161	390910	2	0	0	0	0
162	400890	0	2	0	0	0
163	400900	2	0	0	0	0
164	400910	2	0	0	0	0
165	400920	2	0	0	0	0
166	400930	2	0	1	1	0
167	400940	2	0	0	0	0
168	400950	2	0	0	1	0
169	400960	2	0	0	0	0
170	400970	0	2	0	0	0
171	410911	0	2	0	0	2
172	410920	0	2	0	0	0
173	410921	0	2	0	0	2
174	410930	2	0	0	0	0
175	410931	0	2	0	0	0
176	410940	2	0	0	0	0
177	410950	0	2	0	0	0
178	410951	0	2	0	0	0
179	410960	0	2	0	0	0
180	420920	2	0	0	0	0
181	420930	0	2	0	0	0
182	420940	2	0	0	0	0
183	420950	2	0	1	1	0
184	420960	2	0	0	0	0
185	420970	2	0	0	1	0
186	420980	2	0	0	1	0
187	420990	2	0	0	0	0
188	421000	2	0	0	1	0
189	430970	0	2	0	0	0
190	430971	0	2	0	0	0
191	430990	2	0	1	1	0
192	440960	2	0	0	0	0
193	440970	0	2	0	0	0
194	440980	2	0	0	0	0
195	440990	2	0	0	0	0
196	441000	2	0	0	0	0
197	441010	2	0	1	1	0
198	441020	2	0	0	0	0
199	441030	2	0	0	1	0
200	441040	2	0	0	1	0

Table B.1 *Table continued.*

Number	Nuclide	JEF2.2	EAF3	Cell calculation		Added
				PWR	LMFBR	
201	441050	2	0	0	0	0
202	441060	2	0	0	0	0
203	451021	0	2	0	0	2
204	451030	2	0	1	1	0
205	451050	2	0	1	0	0
206	461020	2	0	0	0	0
207	461030	0	2	0	0	0
208	461040	2	0	0	0	0
209	461050	0	2	0	0	0
210	461060	2	0	0	0	0
211	461070	2	0	0	1	0
212	461080	2	0	0	0	0
213	461090	0	2	0	0	0
214	461100	2	0	0	0	0
215	471061	0	2	0	0	2
216	471070	2	0	0	0	0
217	471081	0	2	0	0	0
218	471090	2	0	1	1	0
219	471101	0	2	0	0	0
220	471110	2	0	0	0	0
221	481060	2	0	0	0	0
222	481080	0	2	0	0	0
223	481090	0	2	0	0	0
224	481100	2	0	0	0	0
225	481110	2	0	0	0	0
226	481120	2	0	0	0	0
227	481130	2	0	1	0	0
228	481131	0	2	0	0	0
229	481140	2	0	0	0	0
230	481150	2	0	0	0	0
231	481151	0	2	0	0	0
232	481160	2	0	0	0	0
233	491130	2	0	0	0	0
234	491141	0	2	0	0	0
235	491150	2	0	0	0	0
236	501120	0	2	0	0	0
237	501130	0	2	0	0	0
238	501140	2	0	0	0	0
239	501150	2	0	0	0	0
240	501160	2	0	0	0	0

Table B.1 *Table continued.*

Number	Nuclide	JEF2.2	EAF3	Cell calculation		Added
				PWR	LMFBR	
241	501170	2	0	0	0	0
242	501171	0	2	0	0	0
243	501180	2	0	0	0	0
244	501190	2	0	0	0	0
245	501191	0	2	0	0	0
246	501200	2	0	0	0	0
247	501210	0	2	0	0	0
248	501211	0	2	0	0	0
249	501220	2	0	0	0	0
250	501230	2	0	0	0	0
251	501240	2	0	0	0	0
252	501250	2	0	0	0	0
253	511201	0	2	0	0	2
254	511210	2	0	0	0	0
255	511220	0	2	0	0	0
256	511230	2	0	0	0	0
257	511240	2	0	0	0	0
258	511250	2	0	0	0	0
259	511260	2	0	0	0	0
260	521191	0	2	0	0	2
261	521200	0	2	0	0	0
262	521210	0	2	0	0	0
263	521211	0	2	0	0	0
264	521220	2	0	0	0	0
265	521230	2	0	0	0	0
266	521231	0	2	0	0	0
267	521240	2	0	0	0	0
268	521250	2	0	0	0	0
269	521251	0	2	0	0	0
270	521260	2	0	0	0	0
271	521270	2	0	0	0	0
272	521271	0	2	0	0	0
273	521280	2	0	0	0	0
274	521290	2	0	0	0	0
275	521291	0	2	0	0	0
276	521300	2	0	0	0	0
277	521311	0	2	0	0	0
278	531250	0	2	0	0	0
279	531260	0	2	0	0	0
280	531270	2	0	1	1	0

Table B.1 *Table continued.*

Number	Nuclide	JEF2.2	EAF3	Cell calculation		Added
				PWR	LMFBR	
281	531280	0	2	0	0	0
282	531290	2	0	1	1	0
283	531300	2	0	0	0	0
284	531310	2	0	0	0	0
285	541240	2	0	0	0	0
286	541250	0	2	0	0	0
287	541260	2	0	0	0	0
288	541270	0	2	0	0	0
289	541280	2	0	0	0	0
290	541290	2	0	0	0	0
291	541291	0	2	0	0	0
292	541300	2	0	0	0	0
293	541310	2	0	1	1	0
294	541311	0	2	0	0	0
295	541320	2	0	0	0	0
296	541330	2	0	0	0	0
297	541331	0	2	0	0	0
298	541340	2	0	0	0	0
299	541350	2	0	1	0	0
300	541360	2	0	0	0	0
301	551310	0	2	0	0	0
302	551330	2	0	1	1	0
303	551340	2	0	1	0	0
304	551350	2	0	1	1	0
305	551360	2	0	0	0	0
306	551370	2	0	0	0	0
307	561300	0	2	0	0	0
308	561310	0	2	0	0	0
309	561320	0	2	0	0	0
310	561330	0	2	0	0	0
311	561331	0	2	0	0	0
312	561340	2	0	0	0	0
313	561350	2	0	0	0	0
314	561351	0	2	0	0	0
315	561360	2	0	0	0	0
316	561370	2	0	0	0	0
317	561380	2	0	0	0	0
318	561390	0	2	0	0	0
319	561400	2	0	0	0	0
320	571370	0	2	0	0	0

Table B.1 *Table continued.*

Number	Nuclide	JEF2.2	EAF3	Cell calculation		Added
				PWR	LMFBR	
321	571380	0	2	0	0	0
322	571390	2	0	1	0	0
323	571400	2	0	0	0	0
324	571410	0	2	0	0	0
325	581360	0	2	0	0	0
326	581371	0	2	0	0	0
327	581380	0	2	0	0	0
328	581390	0	2	0	0	0
329	581400	2	0	0	0	0
330	581410	2	0	0	0	0
331	581420	2	0	0	0	0
332	581430	2	0	0	0	0
333	581440	2	0	0	0	0
334	591410	2	0	1	1	0
335	591420	2	0	0	0	0
336	591430	2	0	0	0	0
337	601420	2	0	0	0	0
338	601430	2	0	1	1	0
339	601440	2	0	0	0	0
340	601450	2	0	1	1	0
341	601460	2	0	1	0	0
342	601470	2	0	0	0	0
343	601480	2	0	0	0	0
344	601490	0	2	0	0	0
345	601500	2	0	0	0	0
346	611450	0	2	0	0	0
347	611470	2	0	1	1	0
348	611480	2	0	1	0	0
349	611481	0	2	0	0	0
350	611490	2	0	1	0	0
351	611500	0	2	0	0	0
352	611510	2	0	0	0	0
353	621440	2	0	0	0	0
354	621450	0	2	0	0	0
355	621460	0	2	0	0	0
356	621470	2	0	1	0	0
357	621480	2	0	0	0	0
358	621490	2	0	1	1	0
359	621500	2	0	1	0	0
360	621510	2	0	1	1	0

Table B.1 *Table continued.*

Number	Nuclide	JEF2.2	EAF3	Cell calculation		Added
				PWR	LMFBR	
361	621520	2	0	1	0	0
362	621530	2	0	0	0	0
363	621540	2	0	0	0	0
364	631501	0	2	0	0	2
365	631510	2	0	0	0	0
366	631520	2	0	0	0	0
367	631521	0	2	0	0	0
368	631530	2	0	1	1	0
369	631540	2	0	1	0	0
370	631550	2	0	1	1	0
371	631560	2	0	0	0	0
372	641520	0	2	0	0	0
373	641530	0	2	0	0	0
374	641540	2	0	0	0	0
375	641550	2	0	0	0	0
376	641560	2	0	0	0	0
377	641570	2	0	0	0	0
378	641580	2	0	0	0	0
379	641590	0	2	0	0	0
380	641600	2	0	0	0	0
381	651570	0	2	0	0	0
382	651590	2	0	0	0	0
383	651600	2	0	0	0	0
384	651610	0	2	0	0	0
385	661560	0	2	0	0	0
386	661570	0	2	0	0	0
387	661580	0	2	0	0	0
388	661590	0	2	0	0	0
389	661600	2	0	0	0	0
390	661610	2	0	0	0	0
391	661620	2	0	0	0	0
392	661630	2	0	0	0	0
393	661640	2	0	0	0	0
394	661650	0	2	0	0	0
395	661660	0	2	0	0	0
396	671630	0	2	0	0	0
397	671650	2	0	0	0	0
398	671660	0	2	0	0	0
399	671661	0	2	0	0	0
400	681620	0	2	0	0	0

Table B.1 *Table continued.*

Number	Nuclide	JEF2.2	EAF3	Cell calculation		Added
				PWR	LMFBR	
401	681640	0	2	0	0	0
402	681650	0	2	0	0	0
403	681660	2	0	0	0	0
404	681670	2	0	0	0	0
405	681680	0	2	0	0	0
406	681690	0	2	0	0	0
407	681700	0	2	0	0	0
408	681710	0	2	0	0	0
409	681720	0	2	0	0	0
410	691690	0	2	0	0	0
411	691700	0	2	0	0	0
412	691710	0	2	0	0	0
413	691720	0	2	0	0	0
414	701680	0	2	0	0	0
415	701690	0	2	0	0	0
416	701700	0	2	0	0	0
417	701710	0	2	0	0	0
418	701720	0	2	0	0	0
419	701730	0	2	0	0	0
420	701740	0	2	0	0	0
421	701750	0	2	0	0	0
422	701760	0	2	0	0	0
423	711741	0	2	0	0	2
424	711750	2	0	0	0	0
425	711760	2	0	0	0	0
426	711770	0	2	0	0	0
427	711771	0	2	0	0	0
428	721740	2	0	0	0	0
429	721750	0	2	0	0	0
430	721760	2	0	0	0	0
431	721770	2	0	0	0	0
432	721780	2	0	0	0	0
433	721790	2	0	0	0	0
434	721800	2	0	0	0	0
435	72180i	0	2	0	0	0
436	721810	0	2	0	0	0
437	721820	0	2	0	0	0
438	731800	0	2	0	0	0
439	731801	0	2	0	0	2
440	731810	2	0	0	0	0

Table B.1 *Table continued.*

Number	Nuclide	JEF2.2	EAF3	Cell calculation		Added
				PWR	LMFBR	
441	731820	2	0	0	0	0
442	731830	0	2	0	0	0
443	741800	0	2	0	0	0
444	741810	0	2	0	0	0
445	741820	2	0	0	0	0
446	741830	2	0	0	0	0
447	741840	2	0	0	0	0
448	741850	0	2	0	0	0
449	741860	2	0	0	0	0
450	741870	0	2	0	0	0
451	741880	0	2	0	0	0
452	751841	0	2	0	0	2
453	751850	2	0	0	0	0
454	751860	0	2	0	0	0
455	751861	0	2	0	0	2
456	751870	2	0	0	0	0
457	751880	0	2	0	0	0
458	751890	0	2	0	0	0
459	761840	0	2	0	0	0
460	761850	0	2	0	0	0
461	761860	0	2	0	0	0
462	761870	0	2	0	0	0
463	761880	0	2	0	0	0
464	761890	0	2	0	0	0
465	761900	0	2	0	0	0
466	761910	0	2	0	0	0
467	761911	0	2	0	0	0
468	761920	0	2	0	0	0
469	761930	0	2	0	0	0
470	761940	0	2	0	0	0
471	771910	0	2	0	0	0
472	771920	0	2	0	0	0
473	771930	0	2	0	0	0
474	771931	0	2	0	0	2
475	771940	0	2	0	0	0
476	771941	0	2	0	0	0
477	781900	0	2	0	0	0
478	781910	0	2	0	0	0
479	781920	0	2	0	0	0
480	781930	0	2	0	0	0

Table B.1 *Table continued.*

Number	Nuclide	JEF2.2	EAF3	Cell calculation		Added
				PWR	LMFBR	
481	781931	0	2	0	0	0
482	781940	0	2	0	0	0
483	781950	0	2	0	0	0
484	781951	0	2	0	0	0
485	781960	0	2	0	0	0
486	781970	0	2	0	0	0
487	781980	0	2	0	0	0
488	791981	0	2	0	0	2
489	791970	2	0	0	0	0
490	791980	0	2	0	0	0
491	791990	0	2	0	0	0
492	792001	0	2	0	0	2
493	801951	0	2	0	0	2
494	801960	0	2	0	0	0
495	801970	0	2	0	0	0
496	801971	0	2	0	0	0
497	801980	0	2	0	0	0
498	801990	0	2	0	0	0
499	802000	0	2	0	0	0
500	802010	0	2	0	0	0
501	802020	0	2	0	0	0
502	802030	0	2	0	0	0
503	802040	0	2	0	0	0
504	812030	0	2	0	0	0
505	812040	0	2	0	0	0
506	812050	0	2	0	0	0
507	822040	0	2	0	0	0
508	822050	0	2	0	0	0
509	822060	0	2	0	0	0
510	822070	0	2	0	0	0
511	822080	0	2	0	0	0
512	822090	0	2	0	0	0
513	832080	0	2	0	0	0
514	832090	2	0	0	0	0
515	832100	0	2	0	0	0
516	832101	0	2	0	0	0
517	842100	0	2	0	0	0
Total	1034	469	565	44	42	32

Table B.2 *Origin of cross sections in the actinide library.*

Number	Nuclide	JEF2.2	EAF3	Cell calculation		Add ed
				PWR	LMFBR	
1	822060	0	2	0	0	0
2	822070	0	2	0	0	0
3	822080	0	2	0	0	0
4	822090	0	2	0	0	0
5	822100	0	2	0	0	0
6	832090	2	0	0	0	0
7	832100	0	2	0	0	0
8	842100	0	2	0	0	0
9	862220	0	2	0	0	0
10	882230	0	2	0	0	0
11	882240	0	2	0	0	0
12	882250	0	2	0	0	0
13	882260	0	2	0	0	0
14	882280	0	2	0	0	0
15	892250	0	2	0	0	0
16	892270	0	2	0	0	0
17	902270	0	2	0	0	0
18	902280	0	2	0	0	0
19	902290	0	2	0	0	0
20	902300	2	0	0	0	0
21	902310	0	2	0	0	0
22	902320	2	0	0	0	0
23	902340	0	2	0	0	0
24	912310	2	0	0	0	0
25	912320	0	2	0	0	0
26	912330	2	0	0	0	0
27	922320	2	0	0	0	0
28	922330	2	0	0	0	0
29	922340	2	0	1	1	0
30	922350	2	0	1	1	0
31	922360	2	0	1	1	0
32	922370	2	0	0	0	0
33	922380	2	0	1	1	0
34	932360	0	2	0	0	0
35	932370	2	0	1	1	0
36	932380	2	0	1	1	0
37	932390	2	0	1	1	0
38	942360	2	0	0	0	0
39	942370	0	2	0	0	2
40	942380	2	0	1	1	0

Table B.2 *Table continued.*

Number	Nuclide	JEF2.2	EAF3	Cell calculation		Added
				PWR	LMFBR	
41	942390	2	0	1	1	0
42	942400	2	0	1	1	0
43	942410	2	0	1	1	0
44	942420	2	0	1	1	0
45	942430	2	0	1	1	0
46	942440	2	0	0	0	0
47	952410	2	0	1	1	0
48	952421	2	0	1	1	0
49	952420	2	0	1	1	0
50	952430	2	0	1	1	0
51	962410	0	2	0	0	2
52	962420	2	0	1	1	0
53	962430	2	0	1	1	0
54	962440	2	0	1	1	0
55	962450	2	0	1	1	0
56	962460	2	0	1	1	0
57	962470	2	0	0	0	0
58	962480	2	0	0	0	0
59	972490	2	0	0	0	0
60	982490	2	0	0	0	0
61	982500	2	0	0	0	0
62	982510	2	0	0	0	0
63	982520	2	0	0	0	0
64	982530	2	0	0	0	0
65	992530	2	0	0	0	0
Total	130	82	48	22	22	4

Table B.3 *Origin of cross sections in the fission product library.*

Number	Nuclide	JEF2.2	EAF3	Cell calculation		Add ed
				PWR	LMFBR	
1	10010	0	2	0	0	2
2	10020	0	2	0	0	2
3	10030	0	2	0	0	0
4	20030	0	2	0	0	2
5	30060	0	2	0	0	2
6	30070	0	2	0	0	2
7	40090	0	2	0	0	2
8	40100	0	2	0	0	2
9	50110	0	2	0	0	2
10	60120	0	2	0	0	2
11	60140	0	2	0	0	2
12	70140	0	2	0	0	2
13	70150	0	2	0	0	2
14	100210	0	2	0	0	2
15	260570	0	2	0	0	2
16	260580	0	2	0	0	2
17	260590	0	2	0	0	2
18	260600	0	2	0	0	2
19	270590	0	2	0	0	2
20	280610	0	2	0	0	2
21	280620	0	2	0	0	2
22	280630	0	2	0	0	2
23	280640	0	2	0	0	2
24	280660	0	2	0	0	2
25	290630	0	2	0	0	2
26	290650	0	2	0	0	2
27	290670	0	2	0	0	2
28	300660	0	2	0	0	2
29	300670	0	2	0	0	2
30	300680	0	2	0	0	2
31	300691	0	2	0	0	2
32	300700	0	2	0	0	2
33	300720	0	2	0	0	0
34	310690	0	2	0	0	2
35	310710	0	2	0	0	2
36	310720	0	2	0	0	0
37	320700	0	2	0	0	2
38	320710	0	2	0	0	2
39	320720	2	0	0	0	0
40	320730	2	0	0	0	0

Table B.3 *Table continued.*

Number	Nuclide	JEF2.2	EAF3	Cell calculation		Added
				PWR	LMFBR	
41	320740	2	0	0	0	0
42	320760	0	2	0	0	0
43	320770	0	2	0	0	0
44	330730	0	2	0	0	2
45	330740	0	2	0	0	2
46	330750	2	0	0	0	0
47	330760	0	2	0	0	0
48	330770	0	2	0	0	0
49	340740	0	2	0	0	2
50	340750	0	2	0	0	2
51	340760	2	0	0	0	0
52	340770	2	0	0	0	0
53	340780	2	0	0	0	0
54	340790	0	2	0	0	0
55	340800	2	0	0	0	0
56	340820	2	0	0	0	0
57	350770	0	2	0	0	2
58	350790	2	0	0	0	0
59	350810	2	0	0	0	0
60	350820	0	2	0	0	0
61	360800	2	0	0	0	0
62	360810	0	2	0	0	0
63	360820	2	0	0	0	0
64	360830	2	0	1	0	0
65	360840	2	0	0	0	0
66	360850	2	0	0	0	0
67	360860	2	0	0	0	0
68	370830	0	2	0	0	2
69	370840	0	2	0	0	2
70	370850	2	0	0	0	0
71	370860	2	0	0	0	0
72	370870	2	0	0	0	0
73	380840	0	2	0	0	2
74	380850	0	2	0	0	2
75	380860	2	0	0	0	0
76	380870	2	0	0	0	0
77	380880	2	0	0	0	0
78	380890	2	0	0	0	0
79	380900	2	0	0	0	0
80	390860	0	2	0	0	2

Table B.3 *Table continued.*

Number	Nuclide	JEF2.2	EAF3	Cell calculation		Added
				PWR	LMFBR	
81	390870	0	2	0	0	2
82	390880	0	2	0	0	2
83	390890	2	0	0	0	0
84	390900	2	0	0	0	0
85	390910	2	0	0	0	0
86	400890	0	2	0	0	2
87	400900	2	0	0	0	0
88	400910	2	0	0	0	0
89	400920	2	0	0	0	0
90	400930	2	0	1	1	0
91	400940	2	0	0	0	0
92	400950	2	0	0	1	0
93	400960	2	0	0	0	0
94	400970	0	2	0	0	0
95	410910	0	2	0	0	2
96	410920	0	2	0	0	2
97	410921	0	2	0	0	2
98	410930	2	0	0	0	0
99	410931	0	2	0	0	0
100	410940	2	0	0	0	0
101	410950	0	2	0	0	0
102	410951	0	2	0	0	0
103	410960	0	2	0	0	0
104	420940	0	2	0	0	2
105	420950	2	0	1	1	0
106	420960	2	0	0	0	0
107	420970	2	0	0	1	0
108	420980	2	0	0	1	0
109	420990	2	0	0	0	0
110	421000	2	0	0	1	0
111	430960	0	2	0	0	2
112	430970	0	2	0	0	2
113	430971	0	2	0	0	2
114	430980	0	2	0	0	2
115	430990	2	0	1	1	0
116	440990	2	0	0	0	0
117	441000	2	0	0	0	0
118	441010	2	0	1	1	0
119	441020	2	0	0	0	0
120	441030	2	0	0	1	0

Table B.3 *Table continued.*

Number	Nuclide	JEF2.2	EAF3	Cell calculation		Added
				PWR	LMFBR	
121	441040	2	0	0	1	0
122	441050	2	0	0	0	0
123	441060	2	0	0	0	0
124	451020	0	2	0	0	2
125	451021	0	2	0	0	2
126	451030	2	0	1	1	0
127	451050	2	0	1	0	0
128	461020	0	2	0	0	2
129	461040	2	0	0	0	0
130	461050	0	2	0	0	0
131	461060	2	0	0	0	0
132	461070	2	0	0	1	0
133	461080	2	0	0	0	0
134	461090	0	2	0	0	0
135	461100	2	0	0	0	0
136	461120	0	2	0	0	0
137	471070	2	0	0	0	0
138	471081	0	2	0	0	0
139	471090	2	0	1	1	0
140	471101	0	2	0	0	0
141	471110	2	0	0	0	0
142	481080	0	2	0	0	0
143	481090	0	2	0	0	0
144	481100	2	0	0	0	0
145	481110	2	0	0	0	0
146	481120	2	0	0	0	0
147	481130	2	0	1	0	0
148	481131	0	2	0	0	0
149	481140	2	0	0	0	0
150	481150	2	0	0	0	0
151	481151	0	2	0	0	0
152	481160	2	0	0	0	0
153	491130	2	0	0	0	0
154	491141	0	2	0	0	0
155	491150	2	0	0	0	0
156	501140	2	0	0	0	0
157	501150	2	0	0	0	0
158	501160	2	0	0	0	0
159	501170	2	0	0	0	0
160	501171	0	2	0	0	0

Table B.3 *Table continued.*

Number	Nuclide	JEF2.2	EAF3	Cell calculation		Added
				PWR	LMFBR	
161	501180	2	0	0	0	0
162	501190	2	0	0	0	0
163	501191	0	2	0	0	0
164	501200	2	0	0	0	0
165	501210	0	2	0	0	0
166	501211	0	2	0	0	0
167	501220	2	0	0	0	0
168	501230	2	0	0	0	0
169	501240	2	0	0	0	0
170	501250	2	0	0	0	0
171	501260	2	0	0	0	0
172	511190	0	2	0	0	2
173	511201	0	2	0	0	2
174	511210	2	0	0	0	0
175	511220	0	2	0	0	0
176	511230	2	0	0	0	0
177	511240	2	0	0	0	0
178	511250	2	0	0	0	0
179	511260	2	0	0	0	0
180	511270	0	2	0	0	0
181	521210	0	2	0	0	2
182	521211	0	2	0	0	2
183	521220	2	0	0	0	0
184	521230	2	0	0	0	0
185	521231	0	2	0	0	0
186	521240	2	0	0	0	0
187	521250	2	0	0	0	0
188	521251	0	2	0	0	0
189	521260	2	0	0	0	0
190	521270	2	0	0	0	0
191	521271	0	2	0	0	0
192	521280	2	0	0	0	0
193	521290	2	0	0	0	0
194	521291	0	2	0	0	0
195	521300	2	0	0	0	0
196	521311	0	2	0	0	0
197	521320	2	0	0	0	0
198	531230	0	2	0	0	2
199	531270	2	0	1	1	0
200	531280	0	2	0	0	0

Table B.3 *Table continued.*

Number	Nuclide	JEF2.2	EAF3	Cell calculation		Added
				PWR	LMFBR	
201	531290	2	0	1	1	0
202	531300	2	0	0	0	0
203	531310	2	0	0	0	0
204	531330	0	2	0	0	0
205	531350	2	0	0	0	0
206	541280	2	0	0	0	0
207	541290	2	0	0	0	0
208	541291	0	2	0	0	0
209	541300	2	0	0	0	0
210	541310	2	0	1	1	0
211	541311	0	2	0	0	0
212	541320	2	0	0	0	0
213	541330	2	0	0	0	0
214	541331	0	2	0	0	0
215	541340	2	0	0	0	0
216	541350	2	0	1	0	0
217	541360	2	0	0	0	0
218	551310	0	2	0	0	2
219	551320	0	2	0	0	2
220	551330	2	0	1	1	0
221	551340	2	0	1	0	0
222	551350	2	0	1	1	0
223	551360	2	0	0	0	0
224	551370	2	0	0	0	0
225	561320	0	2	0	0	2
226	561330	0	2	0	0	2
227	561331	0	2	0	0	2
228	561340	2	0	0	0	0
229	561350	2	0	0	0	0
230	561351	0	2	0	0	0
231	561360	2	0	0	0	0
232	561370	2	0	0	0	0
233	561380	2	0	0	0	0
234	561390	0	2	0	0	0
235	561400	2	0	0	0	0
236	571350	0	2	0	0	2
237	571370	0	2	0	0	2
238	571380	0	2	0	0	0
239	571390	2	0	1	0	0
240	571400	2	0	0	0	0

Table B.3 *Table continued.*

Number	Nuclide	JEF2.2	EAF3	Cell calculation		Added
				PWR	LMFBR	
241	571410	0	2	0	0	0
242	581371	0	2	0	0	2
243	581380	0	2	0	0	2
244	581390	0	2	0	0	2
245	581400	2	0	0	0	0
246	581410	2	0	0	0	0
247	581420	2	0	0	0	0
248	581430	2	0	0	0	0
249	581440	2	0	0	0	0
250	591410	2	0	1	1	0
251	591420	2	0	0	0	0
252	591430	2	0	0	0	0
253	601420	2	0	0	0	0
254	601430	2	0	1	1	0
255	601440	2	0	0	0	0
256	601450	2	0	1	1	0
257	601460	2	0	1	0	0
258	601470	2	0	0	0	0
259	601480	2	0	0	0	0
260	601490	0	2	0	0	0
261	601500	2	0	0	0	0
262	611450	0	2	0	0	2
263	611460	0	2	0	0	2
264	611470	2	0	1	1	0
265	611480	2	0	1	0	0
266	611481	2	0	0	0	0
267	611490	2	0	1	0	0
268	611500	0	2	0	0	0
269	611510	2	0	0	0	0
270	621460	0	2	0	0	2
271	621470	2	0	1	0	0
272	621480	2	0	0	0	0
273	621490	2	0	1	1	0
274	621500	2	0	1	0	0
275	621510	2	0	1	1	0
276	621520	2	0	1	0	0
277	621530	2	0	0	0	0
278	621540	2	0	0	0	0
279	631500	0	2	0	0	2
280	631510	2	0	0	0	0

Table B.3 *Table continued.*

Number	Nuclide	JEF2.2	EAF3	Cell calculation		Added
				PWR	LMFBR	
281	631520	2	0	0	0	0
282	631521	0	2	0	0	0
283	631530	2	0	1	1	0
284	631540	2	0	1	0	0
285	631550	2	0	1	1	0
286	631560	2	0	0	0	0
287	631570	2	0	0	0	0
288	641520	0	2	0	0	0
289	641530	0	2	0	0	0
290	641540	2	0	0	0	0
291	641550	2	0	0	0	0
292	641560	2	0	0	0	0
293	641570	2	0	0	0	0
294	641580	2	0	0	0	0
295	641590	0	2	0	0	0
296	641600	2	0	0	0	0
297	651560	0	2	0	0	2
298	651570	0	2	0	0	2
299	651580	0	2	0	0	2
300	651590	2	0	0	0	0
301	651600	2	0	0	0	0
302	651610	0	2	0	0	0
303	661580	0	2	0	0	2
304	661590	0	2	0	0	2
305	661600	2	0	0	0	0
306	661610	2	0	0	0	0
307	661620	2	0	0	0	0
308	661630	2	0	0	0	0
309	661640	2	0	0	0	0
310	661650	0	2	0	0	0
311	661660	0	2	0	0	0
312	671630	0	2	0	0	2
313	671650	2	0	0	0	0
314	671660	0	2	0	0	0
315	671661	0	2	0	0	0
316	681640	0	2	0	0	2
317	681650	0	2	0	0	2
318	681660	2	0	0	0	0
319	681670	2	0	0	0	0
Total	638	354	284	32	26	172